

PHOTON INDUCED ELECTRON ATTACHMENT(U) GEORGIA TECH  
RESEARCH INST ATLANTA F L EISELE DEC 84  
AFWAL-TR-85-2015 F33615-82-C-2202

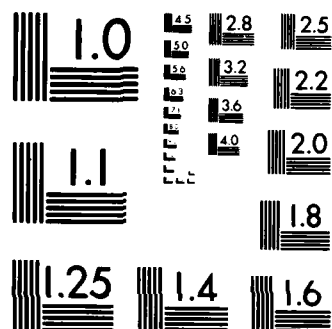
1/1

UNCLASSIFIED

F/G 7/5

NL

UNIVERSITY OF MICHIGAN  
LIBRARY



MICROCOPY RESOLUTION TEST CHART  
NATIONAL BUREAU OF STANDARDS 1062-A



AFWAL-TR-85-2015

PHOTON INDUCED ELECTRON ATTACHMENT

Dr Fred L. Eisele

GEORGIA TECH RESEARCH INSTITUTE  
GEORGIA INSTITUTE OF TECHNOLOGY  
ATLANTA, GEORGIA 30332

DECEMBER 1984

FINAL REPORT FOR PERIOD MAY 1982 - NOVEMBER 1984

APPROVED FOR PUBLIC RELEASE; DISTRIBUTION UNLIMITED.

AERO PROPULSION LABORATORY  
AIR FORCE WRIGHT AERONAUTICAL LABORATORIES  
AIR FORCE SYSTEMS COMMAND  
WRIGHT PATTERSON AIR FORCE BASE, OHIO 45433



85 6 10 022

AD-A156 506

DTIC FILE COPY

NOTICE

When Government drawings, specifications, or other data are used for any purpose other than in connection with a definitely related Government procurement operation, the United States Government thereby incurs no responsibility nor any obligation whatsoever; and the fact that the government may have formulated, furnished, or in any way supplied the said drawings, specifications, or other data, is not to be regarded by implication or otherwise as in any manner licensing the holder or any other person or corporation, or conveying any rights or permission to manufacture use, or sell any patented invention that may in any way be related thereto.


This report has been reviewed by the Office of Public Affairs (ASD/PA) and is releasable to the National Technical Information Service (NTIS). At NTIS, it will be available to the general public, including foreign nations.

This technical report has been reviewed and is approved for publication.

  
PETER BLETZINGER  
Research Engineer  
Power Components Branch

  
PAUL R. BERTHEAUD  
Chief, Power Components Branch  
Aerospace Power Division

FOR THE COMMANDER

  
JAMES D. REAMS  
Chief, Aerospace Power Division  
Aero Propulsion Laboratory

Accession For	
NTIS GRA&I	<input checked="checked" type="checkbox"/>
DTIC TAB	<input type="checkbox"/>
Unannounced	<input type="checkbox"/>
Justification	
By _____	
Distribution/ _____	
Availability Codes	
Dist	Avail and/or Special
A/1	

"If your address has changed, if you wish to be removed from our mailing list, or if the addressee is no longer employed by your organization please notify AFWAL/POOC, W-PAFB, OH 45433 to help us maintain a current mailing list".

Copies of this report should not be returned unless return is required by security considerations, contractual obligations, or notice on a specific document.

## UNCLASSIFIED

SECURITY CLASSIFICATION OF THIS PAGE (When Data Entered)

REPORT DOCUMENTATION PAGE		READ INSTRUCTIONS BEFORE COMPLETING FORM
1. REPORT NUMBER AFWAL-85-2015	2. GOVT ACCESSION NO. 40-A156 506	3. RECIPIENT'S CATALOG NUMBER
4. TITLE (and Subtitle)  PHOTON INDUCED ELECTRON ATTACHMENT		5. TYPE OF REPORT & PERIOD COVERED Final Report May 1982 - November 84
		6. PERFORMING ORG. REPORT NUMBER
7. AUTHOR(s)  F. L. Eisele		8. CONTRACT OR GRANT NUMBER(s)  F33615-82-C-2202
9. PERFORMING ORGANIZATION NAME AND ADDRESS Georgia Tech Research Institute Georgia Institute of Technology Atlanta, Georgia 30332		10. PROGRAM ELEMENT, PROJECT, TASK AREA & WORK UNIT NUMBERS  2301S293
11. CONTROLLING OFFICE NAME AND ADDRESS Aero Propulsion Laboratory (AFWAL/POOC-3) Air Force Wright Aeronautical Lab (AFSC) Wright-Patterson AFB, Ohio 45433		12. REPORT DATE December 1984
		13. NUMBER OF PAGES 55
14. MONITORING AGENCY NAME & ADDRESS (if different from Controlling Office)		15. SECURITY CLASS. (of this report)  Unclassified
		15a. DECLASSIFICATION/DOWNGRADING SCHEDULE
16. DISTRIBUTION STATEMENT (of this Report)  Approved for public release, distribution unlimited.		
17. DISTRIBUTION STATEMENT (of the abstract entered in Block 20, if different from Report)		
18. SUPPLEMENTARY NOTES		
19. KEY WORDS (Continue on reverse side if necessary and identify by block number) Electron Attachment      Optical Pumping, Excitation;      Electron Beam Sustained Plasma Switch, Photo-enhanced Attachment.		
20. ABSTRACT (Continue on reverse side if necessary and identify by block number) Measurements were performed to determine the feasibility of infrared excitation of the molecules $\text{NF}_3$ , $\text{C}_3\text{F}_8$ , $\text{CO}_2$ , $\text{HCl}$ , and $\text{HCN}$ to an excited state with an enhanced electron attachment rate. The former three molecules were optical pumped by a $\text{CO}_2$ laser but no enhanced attachment was observed at any of the laser lines available. The $\text{HCl}$ $v = 0 \rightarrow 2$ transition was directly pumped by, (see reverse side)		

UNCLASSIFIED

SECURITY CLASSIFICATION OF THIS PAGE(When Data Entered)

Optically mixing of 1.06 micron radiation from a Nd:YAG laser with the output of a YAG pumped dye laser at .660 microns. Little or no enhanced attachment was observed suggesting a dissociative electron attachment cross section of less than  $10^{-15}$  cm<sup>2</sup> for HCl(v=2). A similar technique was used to excite HCN(v=2) but no enhanced electron attachment was observed. 24

UNCLASSIFIED

SECURITY CLASSIFICATION OF THIS PAGE(When Data Entered)

## TABLE OF CONTENTS

<u>Section</u>	<u>Page</u>
I INTRODUCTION.....	1
A. Background.....	1
B. Research Objective.....	2
II SELECTION OF GASES CAPABLE OF ENHANCED ATTACHMENT (PHASE I).....	3
A. Selection Criteria.....	3
B. Electron Attachment and Optical Pumping Data.....	5
C. Molecule Selection.....	12
III EXPERIMENTAL APPARATUS.....	15
A. High Voltage Pulsed Electron Beam Source.....	15
B. Plasma Switch.....	17
C. Photo Excitation.....	27
IV EXPERIMENTAL PROCEDURE.....	34
A. Preliminary Studies.....	34
B. CO <sub>2</sub> Laser Excitation.....	38
C. Excitation of HCl and HCN.....	42
V RESULTS AND CONCLUSIONS.....	47
REFERENCES.....	53

## LIST OF ILLUSTRATIONS

<u>Figure</u>	<u>Page</u>
1    Electron gun and associated circuitry and power supplies built for this study.....	16
2    Electron gun current as a function of time. (A) Shows a direct measurement of gun current before the electrons pass through the foil window. (B) Shows the current measured in the switch cell after the electrons pass through the foil window. The measurement was made with less than a torr of N <sub>2</sub> and no electric fields in the switch cell. The slower response times shown in B are believed to be related to ions and elec- trons formed in the small amount of gas remaining in the switch test cell.....	19
3    Electron gun, switch test cell, and accessories.....	20
4    A relatively long switch pulse measured in 740 Torr of N <sub>2</sub> .....	21
5    Front and side view of cathode and electron window assembly.....	22
6    The anode configuration shown in (A) above was used for the majority of this study, while (B) was used to improve the sensitivity for the final HCl and HCN measurements.....	24
7    Gas handling system built for the present study.....	26



# LIST OF ILLUSTRATIONS (Continued)

Figure		Page
8	The experimental configuration used to study NF <sub>3</sub> , C <sub>3</sub> F <sub>8</sub> and CO <sub>2</sub> .....	28
9	Optical parametric oscillator initially constructed in order to obtain 1.5 and 1.7 radiation for the excitation of HCl and HCN.....	30
10	Frequency mixing technique used for the excitation of HCl and HCN.....	32
11	A plot of switch current as a function of time for a field of 1500V/cm and a switch gas (A) N <sub>2</sub> and (B) N <sub>2</sub> containging $1.9 \times 10^{15}$ C <sub>3</sub> F <sub>8</sub> /cm <sup>3</sup> .....	35
12	A plot of switch current as a function of time. In order to detect photo-enhanced attachment, a laser was fired at T <sub>0</sub> and I <sub>-</sub> was compared to I <sub>+</sub> under a variety of experimental parameters.....	37
13	CO <sub>2</sub> laserlines used to study NF <sub>3</sub> , C <sub>3</sub> F <sub>8</sub> and CO <sub>2</sub> .....	39
14	Transmittance of NF <sub>3</sub> as a function of frequency (200 Torr in a 10 cm long cell) from Reference 35. The arrows show the typical CO <sub>2</sub> laser excitation frequencies used for NF <sub>3</sub> photo- enhanced attachment measurements.....	40

LIST OF ILLUSTRATIONS (Concluded)

<u>Figure</u>		<u>Page</u>
15	Transmittance of $C_3F_8$ as a function of frequency (200 Torr in a 10 cm long cell) from Reference 36. The arrows show the typical $CO_2$ laser excitation frequencies used for $C_3F_8$ photo-enhanced attachment measurements.....	41
16	Calculated $HCl^{35}$ $v=0 \rightarrow 2$ overtone spectrum. The intensity of individual levels at different temperatures can be directly compared.....	43

## LIST OF TABLES

		<u>Page</u>
1	Data Used to Evaluate Photo-enhanced Attachment..	6
2	Electron Beam Source Specifications.....	18
3	HCN( $v_3=0 \rightarrow 2$ ) Transition Line and Excitation Wavelength From Reference 37.....	46

## SECTION I

### INTRODUCTION

#### A. Background

The need for very high current high voltage switching devices with fast closing and opening capabilities has led to the development of electron beam controlled plasma switches. These switches can withstand much higher energy loading in the switch medium than devices such as thyratrons because of the higher gas densities used (1-10 atmosphere). Switch closing times can be made relatively short because the conduction electrons produced by ionization of the switch gas medium are formed almost simultaneously throughout the length of the switch gap, and the secondary electron production rate can be increased by increasing the electron beam current. The switch opening process, however, appears to be inherently slower, because the electrons are not easily removed simultaneously throughout the length of the switch in a manner similar to their formation. In a high conductivity low attachment rate switch medium, conduction electron removal after electron beam turn-off is accomplished by ambipolar drift to the conduction electrodes, which is quite slow. Electron-ion recombination is also responsible for additional electron removal, the rate of which depends on the positive ion density and can thus be varied. It, however, is not sufficient to provide fast switch opening times at the switch current levels presently of interest. If a gas which readily attaches electrons were added to the switch medium in sufficient quantity (or similarly, if the recombination rates were of a similar magnitude) a new mechanism for fast electron removal throughout the switch would result, and a more rapid switch opening would be achieved. This fast electron removal, however, would take place continuously while the switch is closed and would greatly reduce the conduction current. This

would greatly reduce the switch efficiency (but not improve the temporal rate of change of switch current during the opening process for a given electron beam current).

If, however, an electron attacher could be introduced only when the switch was to be opened and could be removed before the switch was once again closed, it would shorten the switch opening time but not reduce the switch conduction current. A likely candidate for such an attacher would be a molecule that does not readily attach electrons in its ground state but which could be excited by photons to a state where it would have a much higher electron attachment rate. If the excited molecule were quenched back to its ground state by collisions with the switch gas medium on a time scale slightly faster than the switching repetition rate, it would also not reduce the switch current in the following switch cycle.

#### B. Research Objective

The objective of this study was to identify such a molecule (if it exists) and, if found, to demonstrate its ability to improve the opening time of an electron beam sustained plasma switch.

This task was divided into two phases. The first phase included a literature search and theoretical study to determine the molecules most likely to have the desired characteristics. The second phase consisted of the construction of an apparatus to measure photo-enhanced electron attachment followed by the use of this apparatus to try to observe and study enhanced attachment for the molecules chosen in Phase I.

## SECTION II

### SELECTION OF GASES CAPABLE OF ENHANCED ATTACHMENT (PHASE I)

#### A. Selection Criteria

In order for a gas to have been considered a probable candidate for photo-enhanced electron attachment in a plasma switch environment, it had to meet several requirements. It must not readily attach electrons in its unperturbed (ground) state. Since switch gas pressures are typically an atmosphere and above, three-body reactions are common, so the gas must have a near zero or negative electron affinity. It also must not rapidly undergo dissociative electron attachment. This same molecule, however, must be able to readily attach electrons when in an excited state. Thus, in general, molecules with a dissociative electron attachment threshold that is two or three times the mean electron energy (under switch closed conditions) make likely candidates for enhance attachment. These same molecules, however, must also be difficult to excite to the dissociative or dissociative attachment threshold by electron impact. The selection of a stable molecule with one or more high electron affinity atoms (such as a halogen) will in general remove the problem of direct dissociation, since this will often require 3-4 electron volts more energy than dissociative attachment. The use of atoms such as the halogens also has the added advantage that they form very stable (electron not readily associatively detached), negative ions, and thus they act as a relatively permanent removal mechanism for the captured conduction electrons.

A second set of criteria included were those concerned with optical excitation. Homonuclear diatomic molecules could not be optically excited and therefore were excluded. Direct excitation of metastable electronic levels is also inherently difficult, thus only pumping schemes involving excitation to levels which

would rapidly decay to metastable levels would be considered. Electronic non-metastable levels cannot be used because they have too short a lifetime to attach a significant number of electrons.

Rotational excitation does not in general, involve sufficient energy change and thus our study focused on vibrational excitation. Unfortunately, however, vibrational energy level spacings are also smaller than the mean electron drift energy of interest (1eV) and are thus often easily excited by the conduction electrons. At the same time, optical pumping is made difficult by the fact that a relatively high vibrational excitation is required to approach a dissociative electron attachment threshold well above the mean electron energy. Therefore, when trying to excite the desired high vibrational levels, one either faces a very small absorption cross section for direct pumping or the need for a considerable amount of power for ladder pumping. If ladder pumping is chosen, one must also be careful not to photodissociate the majority of the molecules unless their fragments will also result in a similarly enhanced attachment.

Finally, there were several desirable characteristics which made some molecules more attractive than others. While these characteristics did not constitute a rigid criteria for selecting the most likely molecules for enhanced attachment, they did, in many cases, influence the selection of molecules to be included in our experimental study. Among these desirable characteristics was the ability of a molecule to be excited to the required level with an existing light source. Simple molecules were viewed as more promising than molecules containing a large number of bonds, because it is difficult to keep the majority of the optically pumped energy in the desired bond or bonds, assuming it could be preferentially deposited there initially. Since the time period for vibrational energy redistribution within an individual molecule is typically sub nanosecond, very little time is available

for electron attachment before the energy is distributed to a number of bonds. If sufficient energy were added to a molecule such that many bonds are excited to a 2-3eV dissociative electron attachment threshold, then the molecules will dissociate again before attaching a significant number of electrons because of fast energy redistribution, (or immediate photo dissociation). Since most, if not all, of the vibrational modes of a large molecule could be either directly or indirectly excited by the conduction electrons, the competition between the desired optical and the initially unwanted electron pumping would generally be less favorable in larger molecules.

#### B. Electron Attachment and Optical Pumping Data

The selection of molecular species to be experimentally studied for enhanced electron attachment was made on the basis of the aforementioned criteria and the relevant data available on the most promising molecular species in a variety of categories. Unfortunately, little of the desired information (such as: electron attachment rates for excited molecules, ion-ion recombination rates, electron excitation rates for specific vibrational states, collisional quenching rates between various states or to the ground state, and photo dissociation efficiencies) is known, even for simple molecules like HCl or HF, and nearly none of these quantities have been measured or calculated for the more complex molecules of interest. Thus, in all except a few case (where temperature dependent attachment rates were measured), it was necessary to base our choice of promising photo-enhanced attachers on the fact that a considerably enhanced attachment rate is expected when a molecule is pumped above the dissociative electron attachment threshold, or alternatively on a rapid change in the electron energy dependence of the attachment cross sections. Table 1 shows some of the calculated and experimental data used to evaluate prospective photo-enhanced electron attaching



TABLE 1 Data Used to Evaluate Photo-enhanced Attachment

Gas	Electron Affinity (eV)	Calculated Dissociative Electron Attachment Threshold(eV)	Electron Attachment Cross Section or Rate (the first number is for 300°K unless otherwise noted)	Excitation Method and Estimated Yield
HCl	-0	0.6(19-21)	$<10^{-18} \text{ cm}^2$ @ $<.6 \text{ eV}$ $\sim 5 \times 10^{-18} \text{ cm}^2$ @ $1 \text{ eV}(1,19)$ $8 \times 10^{-15} \text{ cm}^2$ @ $.3 \text{ eV}$ for HCl( $\nu=2$ )(1,19)	YAG:OPO $1.7\mu \sim 20\%$ $\nu=2$ (25,34) (absorption cross section of $10^{-19}$ , 20 mJ of $1.7\mu$ multipassed)
HCN	.001-.01(2,18)	1.8(21),	probably small for $<1.8 \text{ eV}$	YAG:OPO $1.5\mu$ , 20% (26,27) $\nu=2$ (estimate similar to HCl)
COS	.46 $\pm$ 0.2(3)	~0.8(15,21)	$<10^{-18} \text{ cm}^2$ @ $<.7 \text{ eV}$ , $5 \times 10^{-18} \text{ cm}^2$ @ $1 \text{ eV}(4)$ $3 \times 10^{-17} \text{ cm}^2$ @ $1.25 \text{ eV}(4)$	YAG:OPO $4.7\mu$ , 20% $\nu=1$ (26) $2.4\mu$ , 2% $\nu=2$ (28)

TABLE 1 (Continued)

Gas	Electron Affinity (eV)	Calculated Dissociative Electron Attachment Threshold (eV)	Electron Attachment Cross Section or Rate (the first number is for 300°K unless otherwise noted)	Excitation Method and Estimated Yield
CS <sub>2</sub>	1.0 ± 0.2 <sup>(5)</sup>	-2.0 (15,21)	<10 <sup>-20</sup> cm <sup>2</sup> @ <2.8 eV, 3.7 × 10 <sup>-19</sup> cm <sup>2</sup> @ 3.35 eV <sup>(4)</sup>	NO COINCIDENCE
NF <sub>3</sub>		0.7 <sup>(15,22,23)</sup>	<10 <sup>-10</sup> cm <sup>3</sup> /s <sup>(12)</sup> , @ 1 eV (10,11) 300k-500k temp. dependent measurements in 1 atm. N <sub>2</sub> (10)	CO <sub>2</sub> laser 10.4 μ, 100% ν = 1 (29) Multiphoton ladder stepping excitation efficiency to higher levels unknown
HgBr <sub>2</sub>		1-3 eV <sup>(6)</sup>	5 × 10 <sup>-10</sup> cm <sup>3</sup> /s @ (1-5 Td in Ne) <sup>(6)</sup>	Very low frequencies, hard to access; typical of metal halides

TABLE 1 (Continued)

Gas	Electron Affinity (eV)	Calculated Dissociative Electron Attachment Threshold(eV)	Electron Attachment Cross Section or Rate (the first number is for 300°K unless otherwise noted)	Excitation Method and Estimated Yield
I <sub>2</sub>	2,5(3)	0-1ev(11,15)	1.8x10 <sup>-10</sup> cm <sup>3</sup> /s (16), 10 <sup>-16</sup> cm <sup>2</sup> /s @ 1ev(11) temperature dependence (11,15)	No direct way to pump I <sub>2</sub> (30) Small UV absorption cross section (30) UV photo-lysis using flash lamp 1100-1900Å ~20% dissociation. Yield HCl (ν>0) expected but unknown
1,1C <sub>2</sub> Cl <sub>2</sub> H <sub>4</sub>		-0	2x10 <sup>-11</sup> cm <sup>3</sup> /s, 1.5x10 <sup>-9</sup> cm <sup>3</sup> /s @ 0.8ev(7) temperature dependence (20)	
1,2 C <sub>2</sub> Cl <sub>2</sub> H <sub>4</sub>		-0	<10 <sup>-10</sup> cm <sup>3</sup> /s, 2x10 <sup>-10</sup> cm <sup>3</sup> /s @ 0.8ev(7)	

TABLE 1 (Continued)

Gas	Electron Affinity (eV)	Calculated Dissociative Electron Attachment Threshold (eV)	Electron Attachment Cross Section or Rate (the first number is for 300°K unless otherwise noted)	Excitation Method and Estimated Yield
CF <sub>3</sub> Cl		0.4 eV <sup>(7)</sup>	10 <sup>-13</sup> cm <sup>3</sup> /s <sup>(5)</sup> , 3x10 <sup>-11</sup> cm <sup>3</sup> /s @ 0.9 eV <sup>(7)</sup>	UV photolysis using flash <sup>(31)</sup> lamp 1100-1350 Å ~20% dissociation. Expected vibrationally excited CF <sub>3</sub>
BCl <sub>3</sub>		~1.1 (9,23)	2.6x10 <sup>-9</sup> cm <sup>3</sup> /s <sup>(9)</sup> (no pressure dependence 5-15 torr)	CO <sub>2</sub> laser (32,33) 10.4 μ ~100% yield for v=1. Multiphoton ladder stepping up to very high v levels
BF <sub>3</sub>	2.65 <sup>(9)</sup>	11.6 observed <sup>(9)</sup> (~4.0 eV <sup>(9,14)</sup> )	1.4x10 <sup>-11</sup> cm <sup>3</sup> /s <sup>(9)</sup>	No IR COINCIDENCES No absorption λ > 1150 Å

TABLE 1 (Continued)

Gas	Electron Affinity (eV)	Calculated Dissociative Electron Attachment Threshold (eV)	Electron Attachment Cross Section or Rate (the first number is for 300°K unless otherwise noted)	Excitation Method and Estimated Yield
HBr		0.2 (8,21)	$10^{-11} \text{ cm}^3/\text{s}$ , $6 \times 10^{-10} \text{ cm}^3/\text{s}$ @ 1 eV (8)	Nd:YAG-OPO $3.9 \mu\text{m}$ ~80% $\nu=1$ (25) $1.95 \mu\text{m}$ ~10% $\nu=2$
H <sub>2</sub>	-0 (14)	-3.7 eV (21,23)	$< 10^{-15} \text{ cm}^3/\text{s}$ , $10^{-15} \text{ cm}^3/\text{s}$ @ 1 eV (13) large vibrational enhancement (13)	No optical method for vibrational excitation since it is a homonuclear diatomic
CF <sub>4</sub>		2.0 (21)	$10^{-20} \text{ cm}^2$ @ $< 4.0 \text{ eV}$ , $6 \times 10^{-19} \text{ cm}^2$ @ 6.0 eV (15)	No absorption at $\lambda > 1150 \text{ \AA}$ No coincidences in IR

TABLE 1 (Continued)

Gas	Electron Affinity (eV)	Calculated Dissociative Electron Attachment Threshold (eV)	Electron Attachment Cross Section or Rate (the first number is for 300°K unless otherwise noted)	Excitation Method and Estimated Yield
CH <sub>2</sub> Cl <sub>2</sub>		0.2 <sup>(21,24)</sup>	5.4x10 <sup>-13</sup> cm <sup>3</sup> /s, 3.4x10 <sup>-32</sup> cm <sup>6</sup> /s <sup>(17)</sup>	UV photo-lysis using flash (30) lamp: 1100-1950 -50 photo-dissociation. Yield HCl (ν>0) expected but unknown
CH <sub>3</sub> CN	-0.0 <sup>(18)</sup>	1.6 <sup>(21)</sup>	probably small θ < 1.6 eV	YAG:OPO 4.4 μ 20% ν=1 (26) 2.2 μ 2% ν=2
HF	-0.0 <sup>(14)</sup>	2.4 <sup>(21,23)</sup>	probably small θ < 2.4 eV relative temp. dependent measurements <sup>(19)</sup>	HF laser, 2.9 μ 5% ν=1 (25)

molecules. Electron affinities are included in the table because three-body attachment can be an important electron loss process at the high pressures of interest (1-10 atm). A sharp increase in the electron attachment cross section or a dissociative electron attachment threshold of a few eV are considered desirable, (since a few eV would in general be above the mean conduction electron energy). Thus, only the high energy tail of the electron energy distribution would be able to be directly dissociatively attached and initially unwanted electron collisional pumping of the molecule to the threshold level would be small. Unfortunately, optical vibrational pumping to this level is often quite difficult. The absorption wavelength and estimates of the difficulty in exciting the molecule to the desired level is also included in the table. A very small photo absorption cross section and/or a sharp absorption peak where no intense light source is available (such as for HF) can impose an important practical limit on both experimental studies and the applications of certain molecules as enhanced attachers in an electron beam sustained plasma switch.

### C. Molecule Selection

The molecules selected for further study at the end of Phase I of this project were: HCl, HCN,  $\text{NF}_3$ ,  $\text{BCl}_3$ , COS, 1, 2  $\text{C}_2\text{Cl}_2\text{H}_4$  and/or  $\text{CH}_2\text{Cl}_2$ .

A considerable amount of data was available on HCl and it appeared to be a good candidate for photon induced attachment in the low E/N range (electron energies .2-.3eV under switch closed conditions). Its attachment rate is low for 0.2-0.3eV electrons and it is probably not efficiently pumped into high vibrational states by them. HCl can be optically pumped, and was expected to have a greatly increased attachment rate in the second vibrational level. The attaching rate of the ground state molecules was also expected to increase with increasing energy up to about 1.0eV. These desirable characteristics gradually decreased

as the average electron energy distribution approaches 1eV. HCN, a triatomic linear molecule, was expected to be chemically very similar to HCl. Unfortunately very little information on attachment rates and possible enhancement of this rate could be found for HCN. It was calculated to have a near zero electron affinity and therefore three-body electron attachment was expected to be low. Since the calculated dissociative attachment threshold was near 2eV, the two-body attachment rate should be low for an electron energy distribution centered around 1eV. This molecule can be optically pumped to higher vibrational levels where it was expected to exhibit a much (several orders of magnitude) larger attachment rate for 1-2eV electrons.

NF<sub>3</sub> and BCl<sub>3</sub> appeared to be the next most likely candidates. Both have a dissociative attachment threshold around 1eV, and can be readily pumped by the CO<sub>2</sub> laser. Both electron energy dependence and temperature dependent data have been found for NF<sub>3</sub> which supported the probable increase in its electron attaching rate at higher vibrational levels. Less information was found for BCl<sub>3</sub> but it was expected that pumping it to near the dissociate threshold (which should be possible) will greatly increase its attachment rate for 0.2-0.3 eV electrons.

COS was suggested because of its relatively low attachment rate for low energy electrons (in part due to its low electron affinity). It is assumed to have an increased attaching rate if it were optically pumped to lower the threshold value closer to the electron mean energy. The final suggested attaching mechanism was to photo-dissociate a molecule with a low electron attaching rate such as 1,2-C<sub>2</sub>Cl<sub>2</sub>H<sub>4</sub> or CH<sub>2</sub>Cl<sub>2</sub>, to yield a vibrationally excited species in this case HCl\*, which should attach electrons much faster than the parent molecule. The yield of HCl (v>0) for these or similar compounds was not well known but could be studied by optically pumping the switch gas with radiation from flash lamp or a surface spark, and observing infrared



fluorescence.

The above list of selected species was submitted to AFWAL for review and to enable them to select three or more species to be studied in Phase II of this project. AFWAL then made the final selection of HCl, HCN, and  $\text{NF}_3$ , and added to this the two gases  $\text{CO}_2$  and  $\text{C}_3\text{F}_8$  for the Phase II experimental study of photo-enhanced attachment rate.

## SECTION III

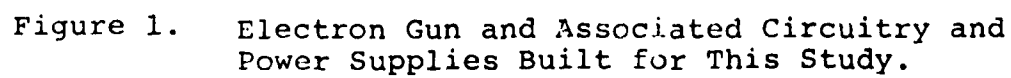
### EXPERIMENTAL APPARATUS

#### A. High Voltage Pulsed Electron Beam Source

A pulsed electron gun was constructed in order to provide a source of conduction electrons in an electron beam sustained plasma switch test cell which could be rapidly turned on and off. Figure 1 shows the electron gun and its control circuitry. Electrons are produced by a heated spiral shaped filament which is housed in a cylindrical metal enclosure. The filament sits immediately behind the only port in this enclosure and is in a plane parallel to it and to the control grid (first grid) shown in Figure 1. In the electron beam "on" state, filament electrons are accelerated rapidly toward the first grid by a strong and near uniform electric field. They then pass through this grid into a near zero field region and subsequently through a second grid, after which they are accelerated to the desired value up to 100 KeV. Finally, they pass through the third grid.

The electron beam is turned off by bringing the control grid to a potential slightly negative with respect to the filament. This prevents the electrons from leaving the filament enclosure. The same new potential is also applied to the deflection plate on the right side of Figure 1, which produces a strong transverse electric field component. This field then deflects any straggling electrons which were between the filament and control grid when the potential was switched, thus shortening the time required for switch turnoff. The electron gun is housed in a vacuum tight enclosure made primarily of stainless steel and ceramics. It is operated in the  $10^{-6}$  torr pressure range which is maintained by a liquid nitrogen trap diffusion pump.

The electron gun and its associated control circuitry is immersed in a high dielectric strength oil bath which provides



both electrical insulation and thermal cooling. The oil is then, in turn water cooled.

A 10 milliamper 100 kV DC supply provides the electron gun potential and the .05 microfarad capacitance bridge provides energy storage for short high current pulses. Power is supplied to the electron gun control circuitry by a 1kVA 100 kV isolation transformer. Thyatron  $T_1$  and grid pulse board 1 were then supplied with the aid of a second low capacitance 20 kV isolation transformer. The control grid was pulsed on and off by thyratrons  $T_1$  and  $T_2$  respectively. When  $T_1$  conducts the charge on the 5000 picofarad capacitor shown in Figure 1, it is shared with the 100 picofarad capacitor, the control grid, and deflection plate thus raising the grid potential to about 12 kV above the filament potential. When  $T_2$  conducts, it reduces the grid and deflection plate potential to about 1 kV below that of the filament, causing the electron beam to be turned off. A negative DC bias is also applied to the control grid between successive pulses to minimize the number of accelerated electrons, which, even if deflected, could still produce unwanted x-rays.

Each of the thyratrons had its own fiber-optically triggered grid driver board which allowed the time and length of the electron beam pulse to be independently selected outside of the high voltage (oil filled) enclosure. Table 2 shows the electrical and temporal operating parameters of our electron beam source, and Figure 2 shows some typical current pulses produced by it.

#### B. Plasma Switch

The plasma switch test cell is shown mounted on the electron beam source in Figure 3 and a typical plot of switch current vs. time is shown in Figure 4. It consists of two stainless steel electrodes, and an insulating glass cell with large optics ports. The cathode electrode is 10 cm in diameter, and has a 4 cm diameter foil window at its center, as shown in Figure 5. A

TABLE 2. Electron Beam Source Specifications

<u>Parameter</u>	<u>Operating Range</u>	<u>Method for Adjusting</u>
electron current	0-300 ma	externally by variac through isolation transformer
electron energy pulsed	20-100 kV	externally by 100 kV power supply variac
electron energy DC	0-100 kV	externally by 100 kV power supply variac
pulse length	1-30 $\mu$ s 10-1000 $\mu$ s	externally by delay generator internally by capacitor and resistor change
pulse repetition rate	0-10 Hertz	externally by delay generator or other trigger source
pulse rise time	$\sim 1 \mu$ s	fixed (can be changed by changing an internal resistor)
pulse fall time	.1-1 $\mu$ s	internal capacitor and resistor change required

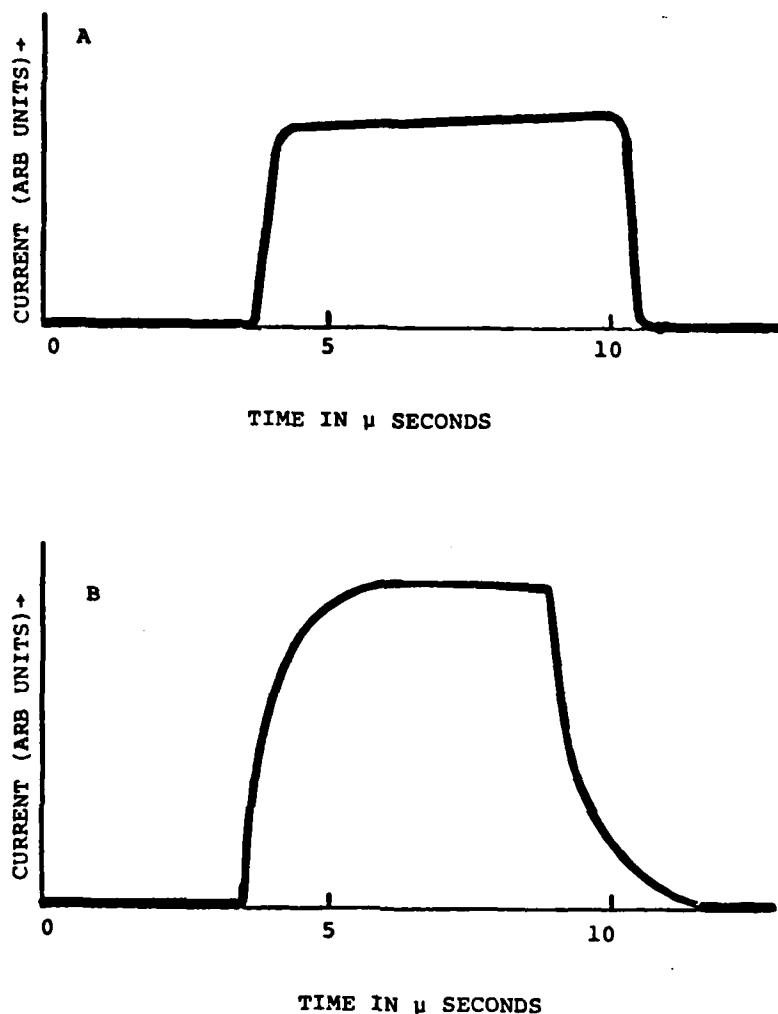


Figure 2. Electron Gun Current as a Function of Time.

(A) Shows a direct measurement of gun current before the electrons pass through the foil window. (B) shows the current measured in the switch cell after the electrons pass through the foil window. The measurement was made with less than a torr of  $N_2$  and no electric fields in the switch cell. The slower response times shown in B are believed to be related to ions and electrons formed in the small amount of gas remaining in the switch test cell.

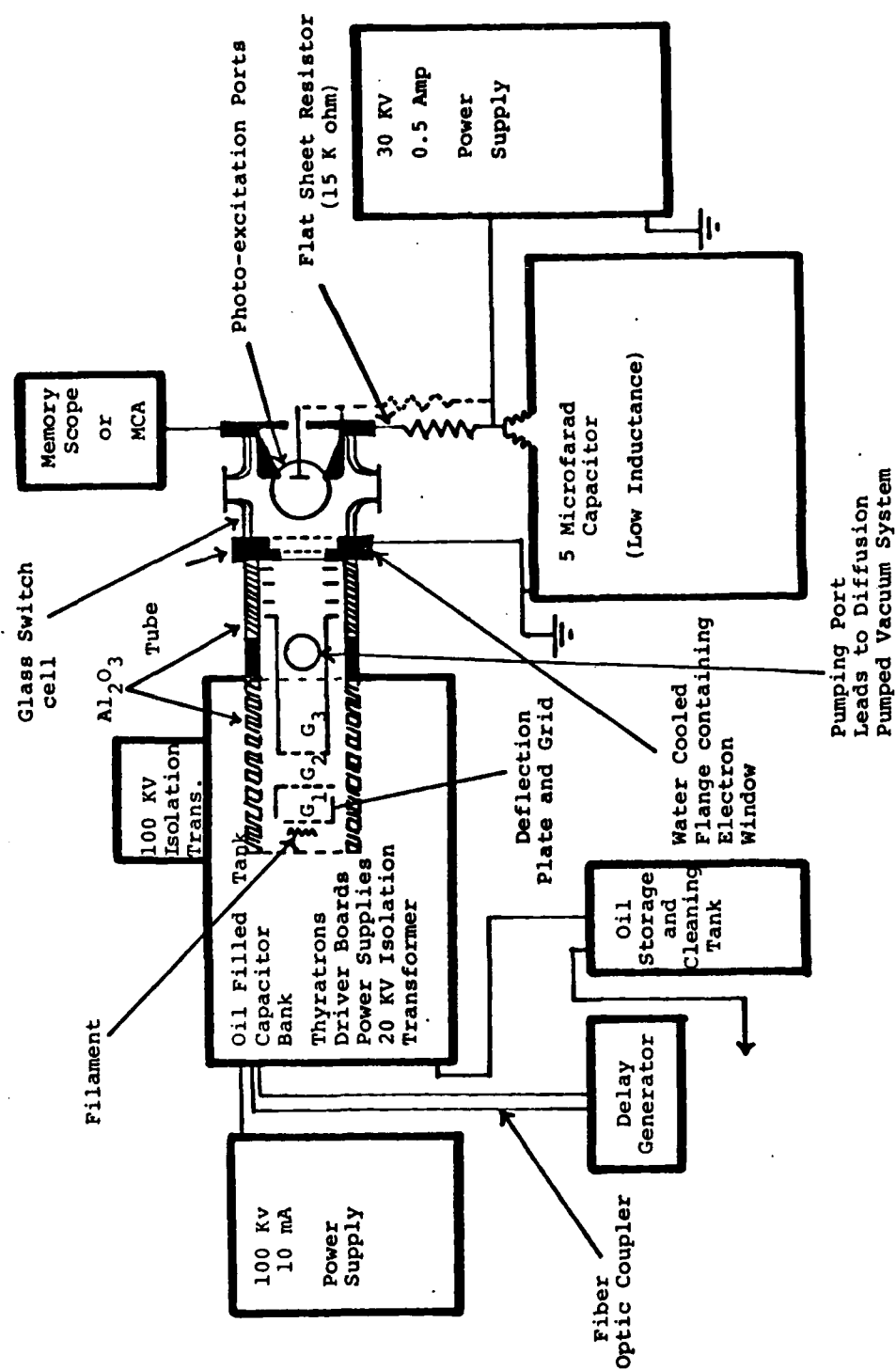


Figure 3. Electron Gun, Switch Test Cell, and Accessories.

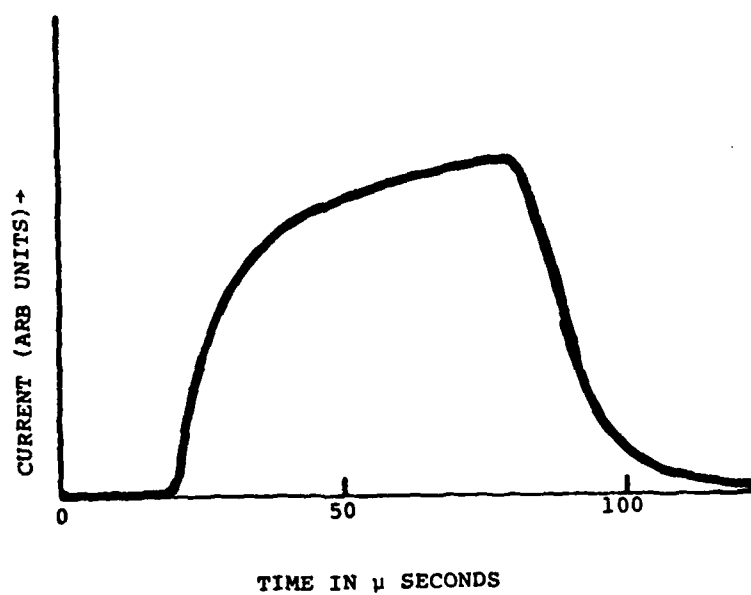


Figure 4. A Relatively Long Switch Pulse Measured  
In 740 Torr of  $N_2$ .



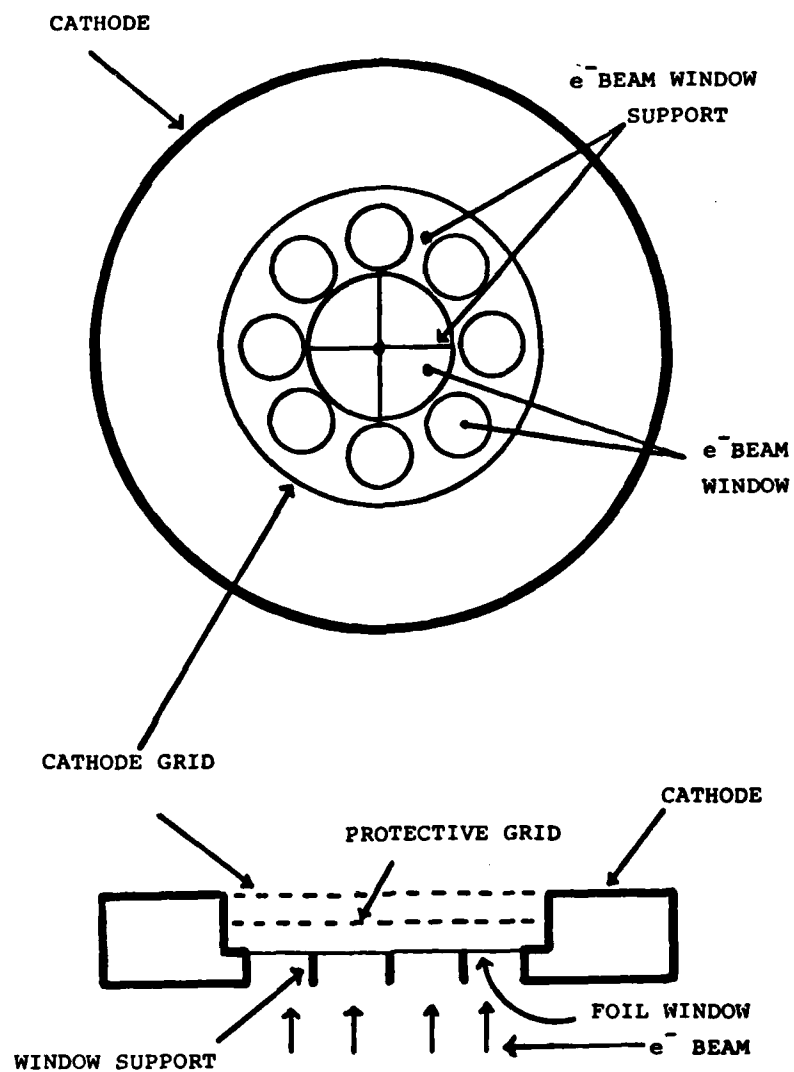


Figure 5. Front and Side View of Cathode and Electron Window Assembly.

stainless steel window was used to separate the electron gun vacuum system from the high pressure test region because of its strength and chemical inertness. The window is 12.5 microns thick and is supported by a high transmittance backing plate. The vacuum seal is made by a Viton O-ring, which allowed the window to be replaced with relative ease. This was of some importance since window breakage was not uncommon. The decision to build a 100 kV electron beam source was a compromise between the difficulty in building a high voltage electron gun and the increased energy loss in the electron window at lower electron energies. Thus, the window was typically under considerable strain and was damaged on several occasions. Two coarse highly transmitting grids were placed on the switch side of the electron window in order to prevent the high switch conduction current from additionally heating the electron window. The anode is about 9 cm in diameter and has a coaxial, electrically isolated center electrode, as shown in Figure 6A. The small central electrode only received a small fraction of the total switch current, but the region in front of it could be more completely filled by excitation photons. A second anode configuration shown in Figure 6B was used in the final portion of this study in order to improve our ability to detect very small photo induced changes in the switch current. This electrode, while decreasing the electric field uniformity, allowed the majority of the switch current to pass through a long narrow region of the test cell which could be optimally photo-excited by a multipassed laser beam.

The region between the electrodes was enclosed by a pyrex cell with two opposing 5 cm diameter windows for optical excitation and two 2.5 cm diameter observation ports. Sodium chloride and quartz windows were used on the excitation ports for 9-11 and 1.5 to 1.7 micron wavelengths respectively. While the sodium chloride windows transmit well at both wavelengths, their surface quality in moist air is far more difficult to maintain. Since

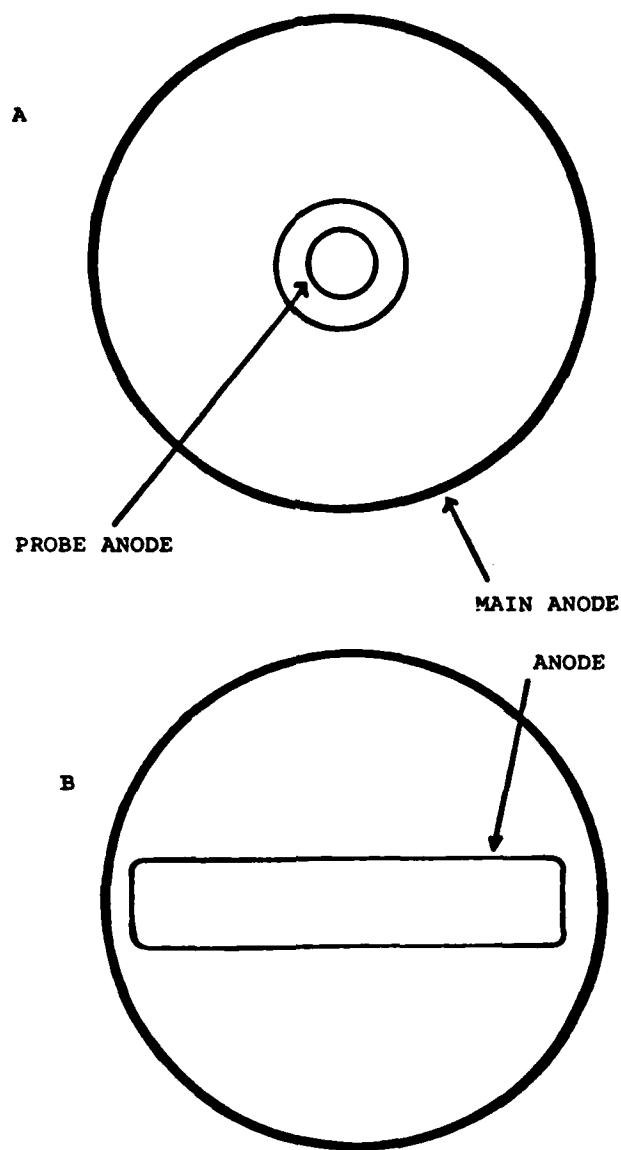


Figure 6. The anode configuration shown in (A) above was used for the majority of this study, while (B) was used to improve the sensitivity for the final HCl and HCN measurements.

quartz does not suffer from this problem, it was used where possible, particularly for the multi-passed beam measurements where light scattered from a slightly rough surface can result in a major loss of power.

Electrical power was supplied to the switch by 15 cm wide copper conductors terminating at a low inductance 5 microfarad capacitor. The load resistors were made from a large number of carbon resistors connected in a series/parallel array to form a flat, wide, low inductance sheet. The charge on the 5 microfarad storage capacitor was maintained by a 0-30 kV, 0.5 ampere DC power supply.

A stainless steel gas handling system capable of safely handling toxic and corrosive gases such as HCN, HCl, and  $\text{NF}_3$  was also constructed. This system is shown in Figure 7, along with the associated monitoring instrumentation. The major switch gas component, typically ultra high purity nitrogen (99.999%), was admitted to the gas handling system through a leak valve at a rate which was monitored by a mass flow meter. A mixture of the attaching gas and nitrogen was admitted in a similar manner, but at a flow rate generally one to three orders of magnitude less than that of the pure nitrogen. The two gases were then combined in a 0.5 liter mixing chamber and flowed out of the exhaust hood area and into the switch test cell. After leaving the switch cell, the gas is again returned to the exhaust hood area. The gas pressure is monitored at the outlet port of the test cell and can be varied from less than a torr to above 1 atmosphere of pressure. Pressures slightly above 1 atmosphere were used to minimize the possibility of unwanted impurities, such as water or oil vapor, getting into the switch particularly from the exhaust port. For safety reasons, measurements with HCN were conducted at slightly less than atmospheric pressure.

Several additional safety precautions were also required, because of the high voltages used and the x-rays produced in and

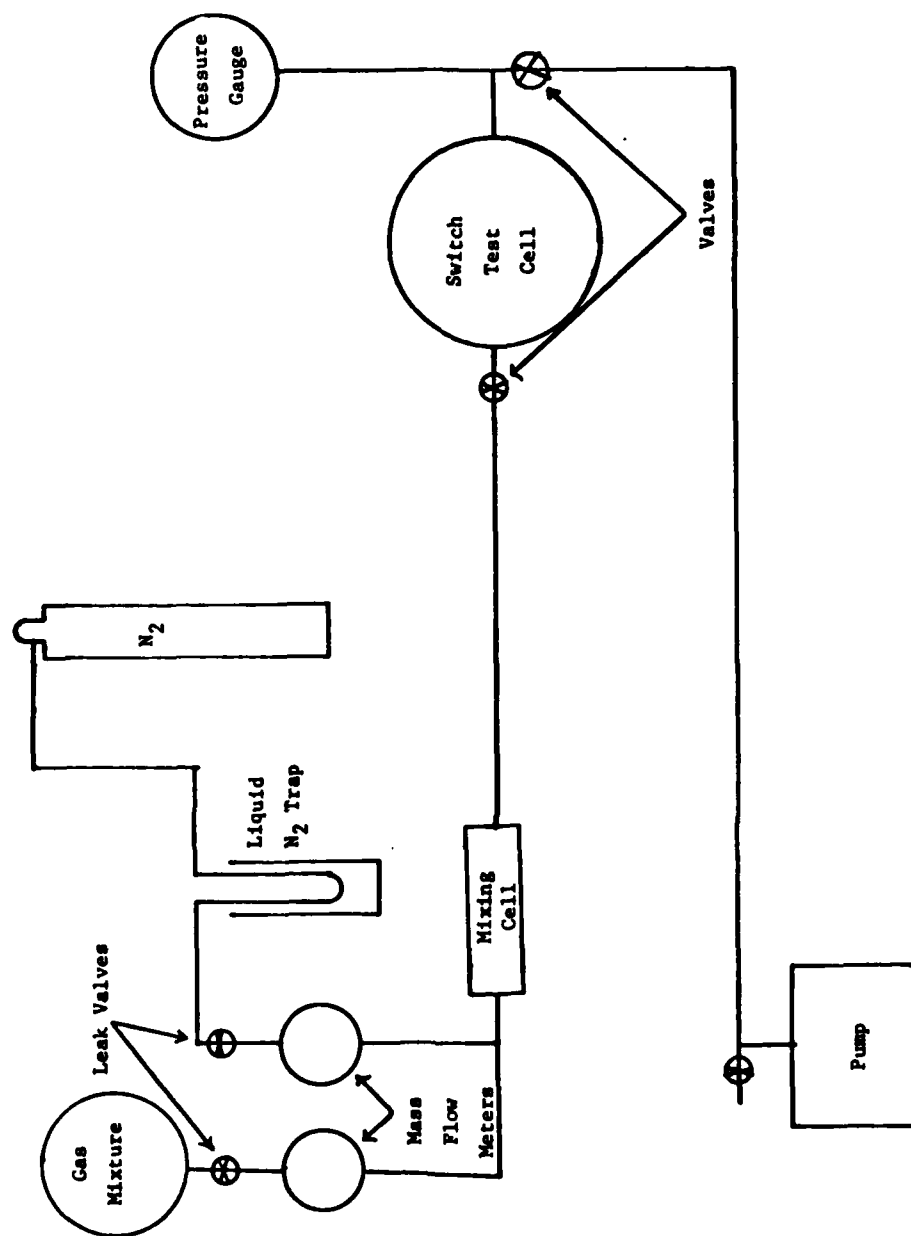


Figure 7. Gas Handling System Built for Present Study.

around the switch cell area. A 3 mm thick lead enclosure was fabricated around the electron gun, its control circuitry and the switch cell. Additional shielding was also added near the window end of the electron gun. The shield around the switch cell was constructed so that it could be easily removed to gain access to the switch cell, load resistor and electrical probes. This removable portion of the shield also contained two ports for optical excitation. Several interlocks were installed under this shield to insure that the electron gun/x-ray source was immediately shut off and the switch storage capacitor rapidly discharged if and when this shield was removed.

Many additional safety and practical devices also had to be built and operated for this experimental study. These devices include a vacuum interlock to isolate the electron gun and diffusion pump in case of pump failure or electron window breakage, as well as to turn off the electron gun filament and associated circuitry and liquid nitrogen. An interlocked x-ray warning light also had to be built. The high dielectric strength oil used to insulate the electron gun also required special care and handling. The performance of this oil is degraded if it is exposed to moist air for extended periods, thus its enclosure had to be sealed and flushed with dry nitrogen. A vacuum tight storage tank and exchange system also had to be installed to allow removal of the oil from around the electron gun and circuitry when repairs were needed. Various additional electronic circuitry also had to be built and tested.

### C. Photo Excitation

Two different wavelength ranges were experimentally studied using quite different techniques. The first method was experimentally quite simple, but involved a far more complex multi-step molecular excitation scheme. A CO<sub>2</sub> laser was used in this study, as shown in Figure 8. It was reflected by an aluminum first

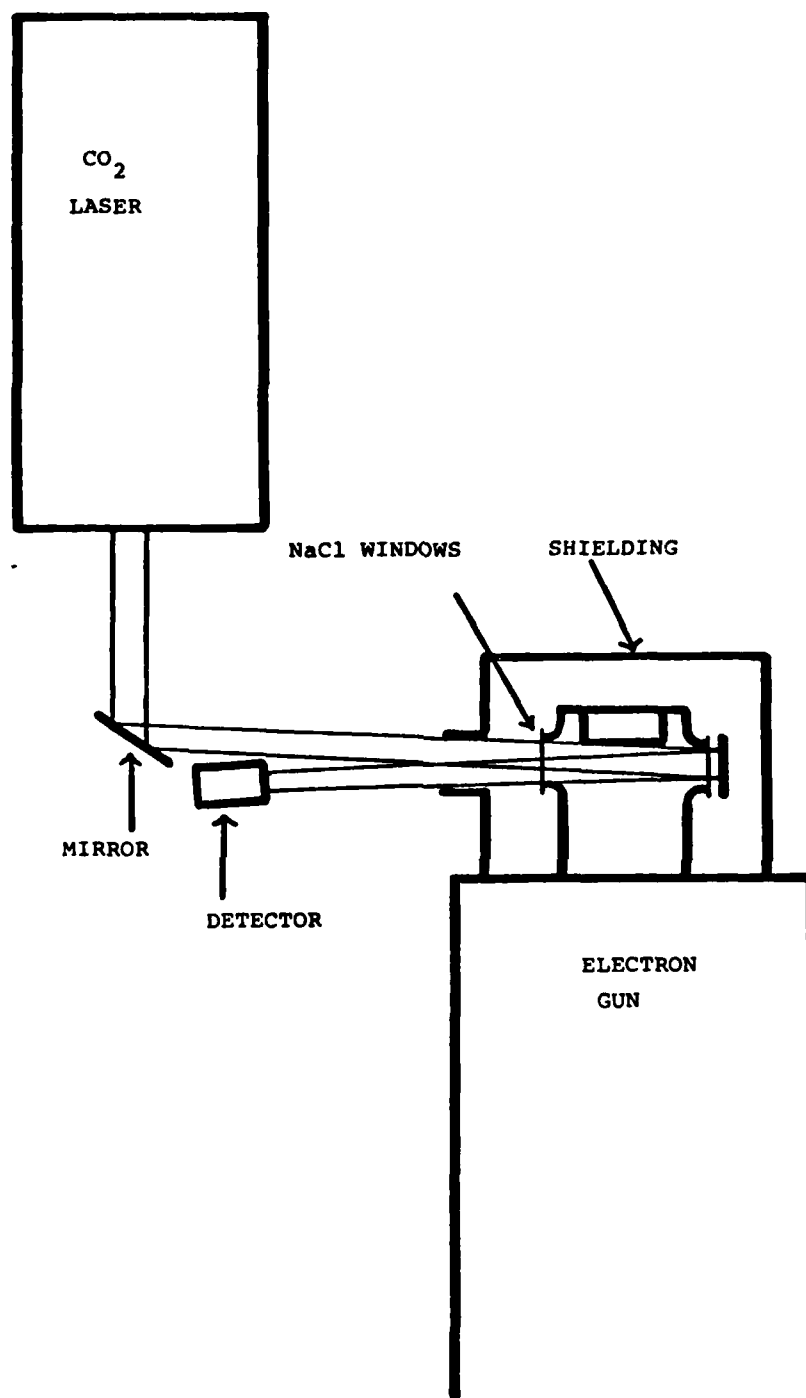


Figure 8. The Experimental Configuration Used to Study  $\text{NF}_3$ ,  $\text{C}_3\text{F}_8$ , and  $\text{CO}_2$ .

surface steering mirror so as to pass through the port in the lead shielding and both test cell windows. It was then reflected by a second aluminum mirror, back through the cell, thus making nearly twice the incident beam energy available for excitation. The laser beam then exited the shielded area and its intensity was measured by an energy monitor. This beam filled an area about 2.5 cm wide across the entire surface of the anode and out to 1.5 cm in front of it. This accounted for the entire area through which the current must flow to reach the central probe anode, and probably an area containing about half the total switch current. The energy density in this area was approximately one joule/cm<sup>2</sup> for the stronger CO<sub>2</sub> lines and was contained in a 200 nanosecond pulse.

Optical excitation experiments in the 1.5-1.7 micron range were far more complex, since there were no intense light sources available in this wavelength range. Our initial attempt at obtaining a light source in this range involved the construction of an optical parametric oscillator (OPO) which by itself is a substantial project. OPOs are not available commercially, and there are only a few in operation within the country, despite their having been virtually the only tunable and relatively intense (several millijoules) light sources in this wavelength range. The operation of the OPO depends on the nonlinear optical properties of a lithium niobate (LiNbO<sub>3</sub>) crystal, which allows a fixed frequency photon to generate two selectable frequency photons, the sum of whose frequencies must equal the incident photon frequency. Unfortunately, the operating threshold of this crystal is very close to its damage threshold, thus requiring a very spatially uniform beam from the Nd:YAG pumping laser. In order to improve the spatial uniformity and remove high intensity spots in the pump beam, it was multipassed several times as shown in Figure 9. The far field beam (10-20 meters) was then used to pump the OPO.



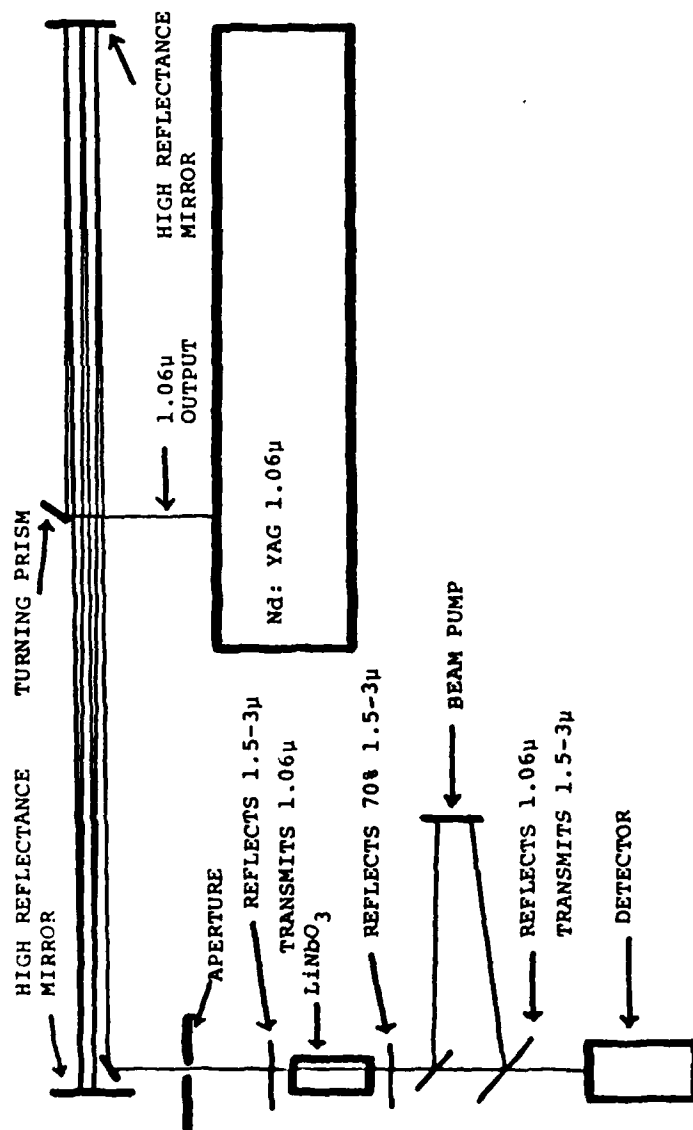


Figure 9. Optical Parametric Oscillator initially constructed in order to obtain 1.5 and 1.7μ radiation for the excitation of HCl and HCN.

Our initial OPO was optically pumped by a Nd:YAG laser with a relatively poor beam uniformity, because it was the only such laser available at that time. A small amount of infrared energy was obtained from the device after considerable effort, but the crystal was finally damaged by hot spots in the laser pump beam. A second YAG laser with a considerably more uniform and stable beam profile soon became available for this study. A new, much larger lithium niobate crystal was then purchased and installed in the OPO. A small amount of infrared power was again obtained from the OPO, but the coating on the new crystal appeared to be defective. The crystal was then returned to the manufacturer, who tried to recoat the crystal to meet the original specifications. After some time it became apparent that the original specification could not be met within a reasonable time frame, and the crystal was returned to the manufacturer for reimbursement.

Advances in nonlinear optics technology by this time had made available a second possible method for obtaining several millijoules of tunable infrared power in the desired wavelength range. This alternative method was quite attractive, since it had by then become commercially available and could be optically pumped by two lasers already available in our lab. The new method of obtaining the desired wavelength was still difficult and required the mixing of the fundamental frequency of the YAG laser with the output of a dye laser, which was pumped by the second harmonic frequency from the same YAG laser. The two frequencies were then mixed in a lithium niobate crystal (at much lower power densities than in the OPO) to give photons at a frequency equal to the difference in the two pump beam frequencies as shown in Figure 10. Tunability of the infrared output was achieved by tuning the dye laser frequency, which was being mixed with the fixed frequency YAG photons. The output line width is controlled by the line width of both lasers, and was narrowed to about  $0.2 \text{ cm}^{-1}$  by installing an etalon in both the YAG and dye lasers. The

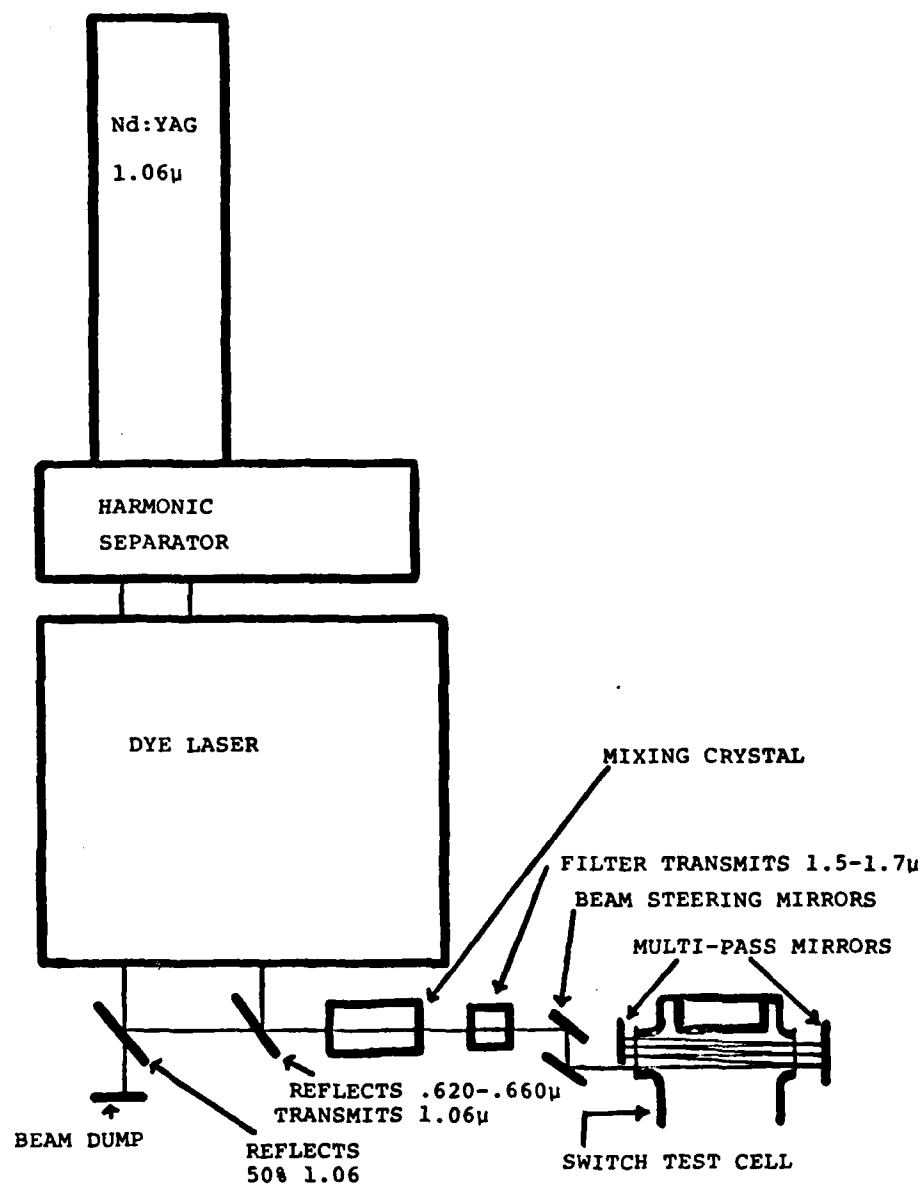


Figure 10. Frequency Mixing Technique Used for the Excitation of HCl and HCN.

maximum power available at 1.5 and 1.7 micron wavelengths from the frequency mixing apparatus was about 2 millijoules in a 7 nanosecond pulse.

## SECTION IV

### EXPERIMENTAL PROCEDURE

#### A. Preliminary Studies

Before photo-excitation measurements could be efficiently carried out, studies of switch operation in the absence of external optical excitation were desirable. These initial studies would then be used to determine the experimental conditions believed most promising for optical excitation measurements.

One of the first observations made in the initial measurements was that high switch currents and long pulse durations appear to lead to substantially enhanced attachment rates in  $C_3F_8$ . Figure 11A shows a plot of the plasma switch current as a function of time for a rather long pulse in nitrogen. Figure 11B shows a plot made under similar conditions, but with  $1.9 \times 10^{15}$   $C_3F_8$  molecules/cm<sup>3</sup> added to the switch gas mixture. The initial current rise is comparable in both plots, but the current soon decreases in the  $C_3F_8/N_2$  mixture, suggesting that the conduction electrons are probably exciting and/or dissociating a sizable portion of the  $C_3F_8$ , which is then in turn leading to enhanced attachment. In order to minimize the competition between internally produced enhanced electron attachment and external photo-excitation enhanced attachment, it was decided to perform our initial studies at very low switch currents, where the electron induced enhanced attachment would be minimal. When significant photo enhancement was then observed and optimized, higher switch currents could be used to study the switch opening processes more fully. Low switch currents also allowed a longer, more uniform, and more reproducible switch pulse to be generated, which improved the sensitivity of our measurements.

The range of test gas concentrations to be used for the optical excitation measurements was also determined from the non-

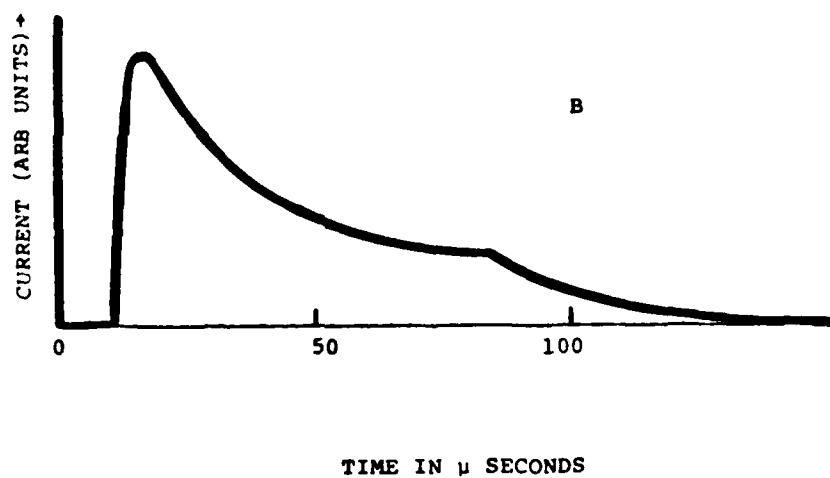
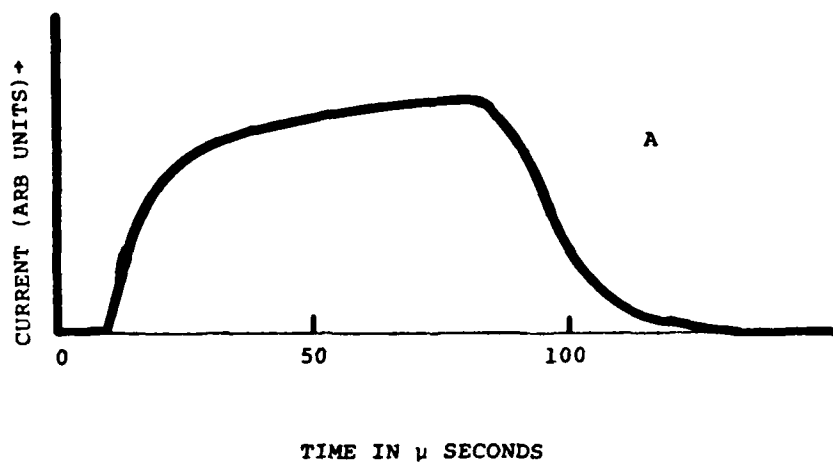


Figure 11. A plot of switch current as a function of time for a field of 1500V/cm and a switch gas of (A)  $N_2$  and (B)  $N_2$  containing  $1.9 \times 10^{15} C_3F_8/cm^3$ .

optical excitation studies. During such studies we became aware of additional experimental problems which had to be solved. The attachment rate of HCl, for example, appeared to be considerably greater than expected at low electric field strengths. This was particularly true if the HCl/N<sub>2</sub> mixture was stored for extended periods before use. The increased attachment was attributed to surface reactions in the gas handling system, which probably resulted in Cl<sub>2</sub> production that could rapidly attach low energy electrons for which the HCl cross section was small. These findings resulted in a modification of the gas handling system and experimental procedures. A teflon gas inlet line which could be used instead of the stainless steel line was added to minimize catalytic surface reactions and the HCl was purified by distillation shortly before its use. Attempts to observe photo-enhanced attachment were then begun, making use of information gained in these initial studies.

Since no enhancement was initially measured, experimental procedures were based on improving our sensitivity for its detection. Instead of trying to observe a small, possibly short lived change in the rate of current decline after electron beam turn off, optical excitation was typically attempted on the flat portion of the switch current-vs-time plot, as shown in Figure 12. It was believed that this, in conjunction with the use of low switch current densities as previously discussed (less than  $10^{-4}$  A/cm<sup>2</sup>), would offer the maximum sensitivity for detecting enhanced attachment. Thus, virtually all of our studies were conducted under these conditions, with only a few brief attempts to observe enhanced attachment during the switch opening time period.

#### B. CO<sub>2</sub> Laser Excitation

The photon enhanced attachment of the three gases NF<sub>3</sub>, C<sub>3</sub>F<sub>8</sub> and CO<sub>2</sub> were all studied in a similar manner, using a pulsed CO<sub>2</sub>

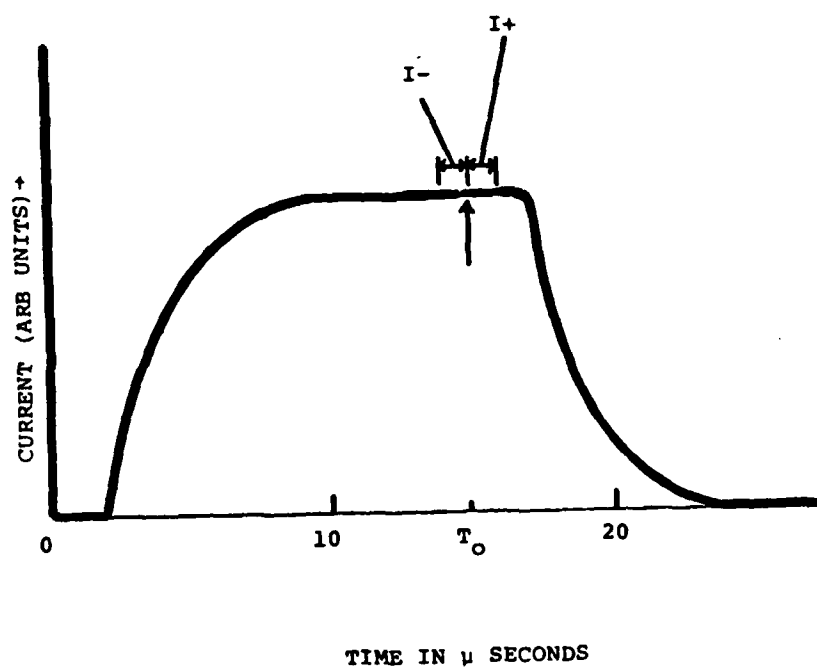


Figure 12. A plot of switch current as a function of time. In order to detect photo-enhanced attachment, a laser was fired at  $T_0$  and  $I_-$  was compared to  $I_+$  under a variety of experimental parameters.



laser as was previously described and shown in Figure 8. The laser used could be tuned to 73 different lasing frequencies, as shown in Figure 13. Each of the three gases was studied at all 73 frequencies, though the majority of measurements were performed for laser frequencies near the absorption peak of the gas. Figure 14 shows the transmittance of  $\text{NF}_3$  as a function of frequency in the infrared wavelength range of interest. Most of the  $\text{NF}_3$  studies were therefore conducted close to the peak absorptions at 907 and 1031  $\text{cm}^{-1}$ . The larger of the two absorption peaks at 907  $\text{cm}^{-1}$  could not be reached, but the absorption appeared to remain quite high in the near proximity, so measurements were conducted in the 921-935  $\text{cm}^{-1}$  range. Measurements were also performed on both sides of the second peak from 1020-1042  $\text{cm}^{-1}$ . The electric field was varied from 23-2600 V/cm and the  $\text{NF}_3$  concentration was varied from  $9.2 \times 10^{13}$ - $2.6 \times 10^{16}/\text{cm}^3$  for the measurements near both absorption peaks, but no photo-enhanced attachment was observed. The lower and upper  $\text{NF}_3$  concentrations limits studied correspond to the values for which only a slight increase in attachment is noted and to an amount which causes a reduction of switch current by about a factor of 10 respectively. A similar criteria was used for determining the test range for the other gas.

A plot of the transmittance of  $\text{C}_3\text{F}_8$  as a function of frequency is shown in Figure 15. Again, the peak of the  $\text{C}_3\text{F}_8$  absorption could not be used for excitation but optical pumping on both sides of and close to the peak at 979-986  $\text{cm}^{-1}$  and 1020-1042  $\text{cm}^{-1}$  should still be quite efficient. The  $\text{CO}_2$  laser lines within the two ranges listed were then used to excite  $\text{C}_3\text{F}_8$  in the switch cell at concentrations of  $3.2 \times 10^{14}$ - $2.1 \times 10^{18}/\text{cm}^3$  and at electric field strengths of 23-2600 V/cm, (limited by strong attachment at higher fields). Again, no photo-enhanced electron attachment could be measured.

Finally, an attempt to observe enhanced attachment in  $\text{CO}_2$

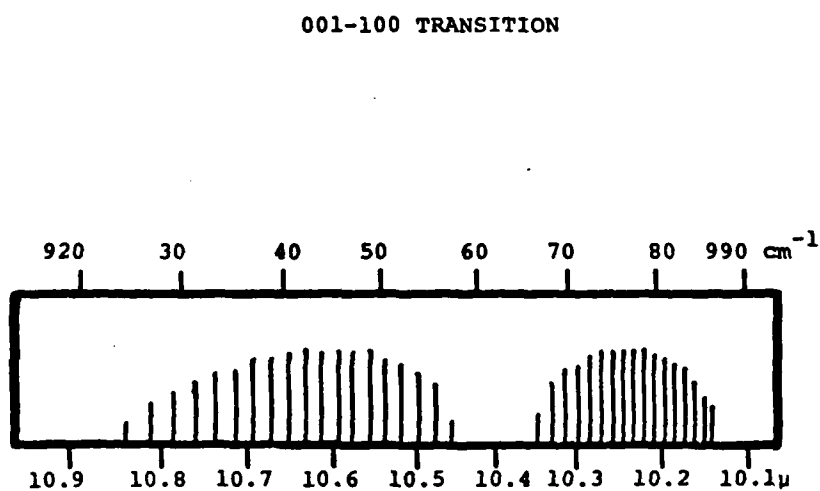
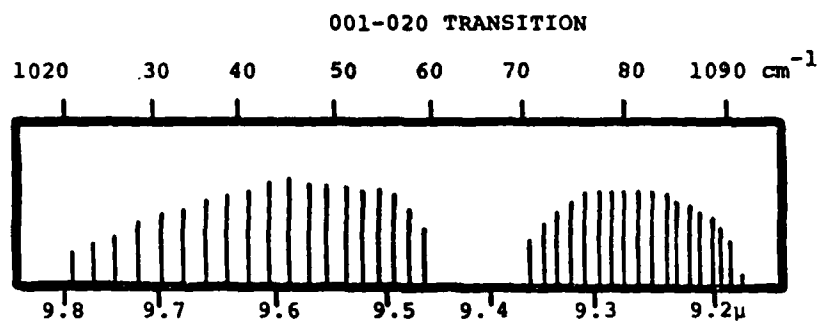


Figure 13.  $\text{CO}_2$  Laser Lines Used to Study  $\text{NF}_3$ ,  $\text{C}_3\text{F}_8$  and  $\text{CO}_2$ .

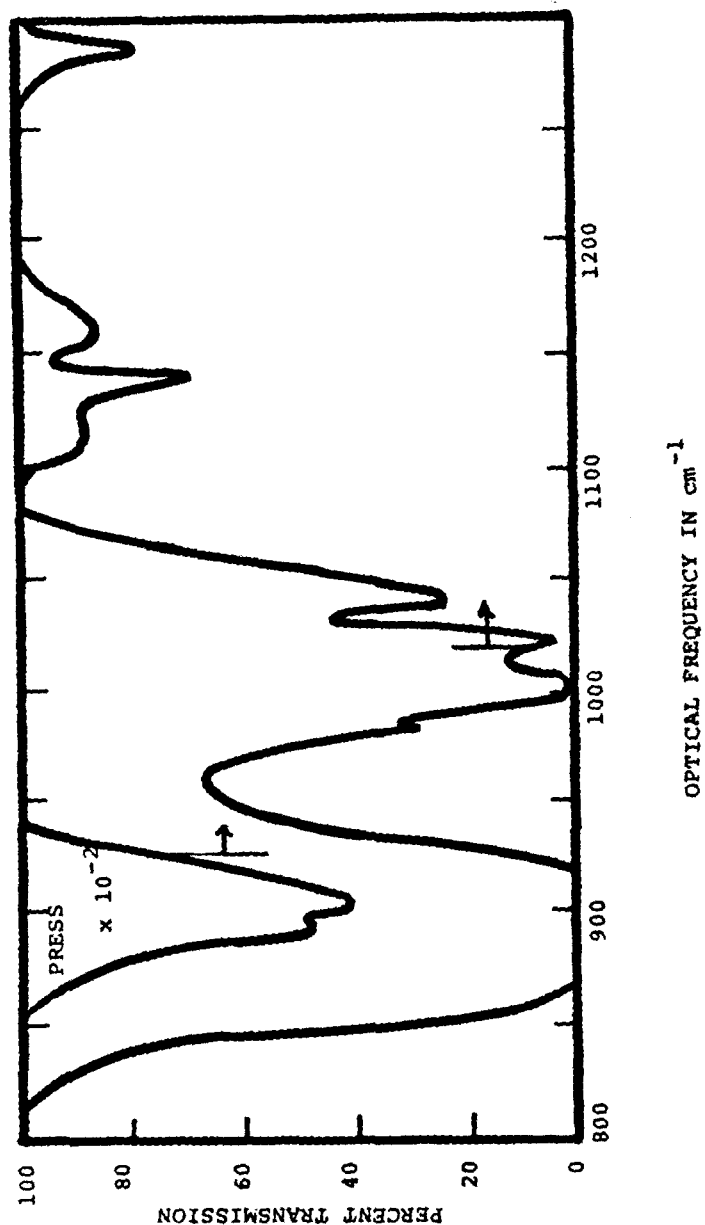


Figure 14. Transmittance of  $\text{NF}_3$  as a function of frequency (200 Torr in a 10 cm long cell) from Reference 35. The arrows show the typical  $\text{CO}_2$  laser excitation frequencies used for  $\text{NF}_3$  photo-enhanced attachment measurements.

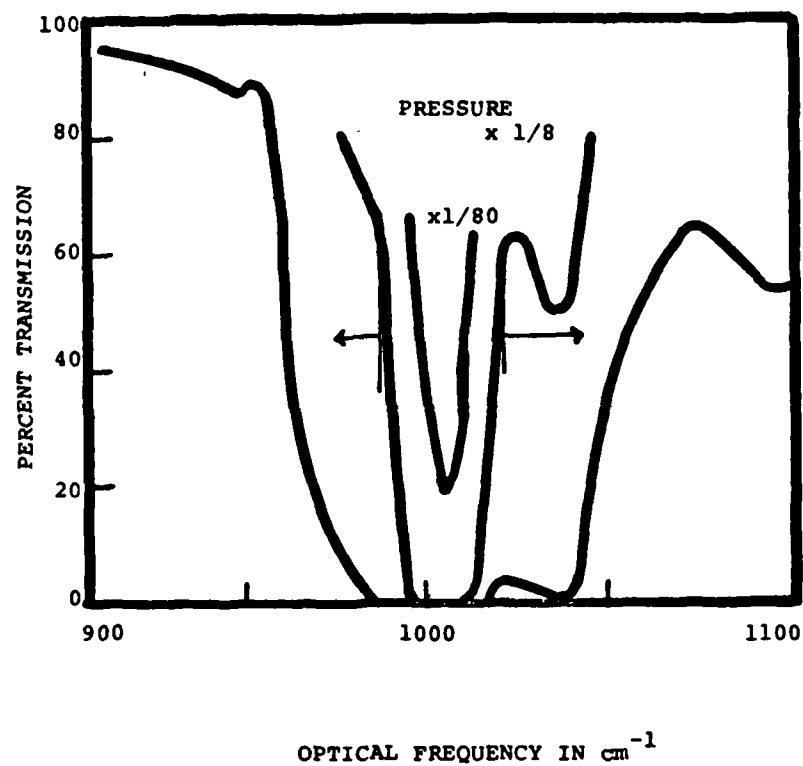


Figure 15. Transmittance of  $C_3F_8$  as a function of frequency (200 Torr in a 10 cm long cell) from Reference 36. The arrows show the typical  $CO_2$  laser excitation frequencies used for  $C_3F_8$  photo-enhanced attachment measurements.

was undertaken.  $\text{CO}_2$  does not have a significant ground state absorption cross-section at an infrared or visible wavelength that is accessible with a substantial amount of optical power (neither of the two  $\text{CO}_2$  laser transitions goes to the ground state, and no accidental overlap with other laser transitions occurs). If, however, the  $\text{CO}_2$  were excited thermally or by collisions with electrons, it might then be excited further by intense  $\text{CO}_2$  laser radiation. Since its optical absorption in one of many possible excited states is unknown, all of the  $\text{CO}_2$  laser wavelengths were used.  $\text{CO}_2$  was studied at electric field strengths of  $100\text{--}2600\text{ V/cm}^3$  and at a concentration of  $2.7 \times 10^{19}$  (no ground state attachment) at all 73 laser frequencies. However, no enhanced attachment was observed.

#### C. Excitation of HCl and HCN

Photons for exciting HCl and HCN were obtained from the tunable laser system shown in Figure 10 and discussed previously. Unlike the  $\text{CO}_2$  laser which has a large number of fixed output wavelengths, this system is continuously tunable, but only provided about  $10^{-4}$  times the number of photons. Those species it is intended to excite, particularly HCl have very narrow absorptions which are widely separated as shown in Figure 16. Therefore, considerable care must be taken to insure that the laser output is sufficiently narrow and at the proper frequency to efficiently excite the HCl molecules. In order to accomplish this an absorption cell with quartz windows was filled with HCl and the infrared output tuned until maximum absorption was observed. The absorption peak used for this study was the largest one shown in Figure 16 in the R branch at  $5753\text{ cm}^{-1}$ . The maximum measured absorption was about 50%, and was nearly independent of HCl pressure above 400 Torr, indicating that the laser line width obtained at 1.7 was at least twice the width of the pressure broadened HCl absorption.

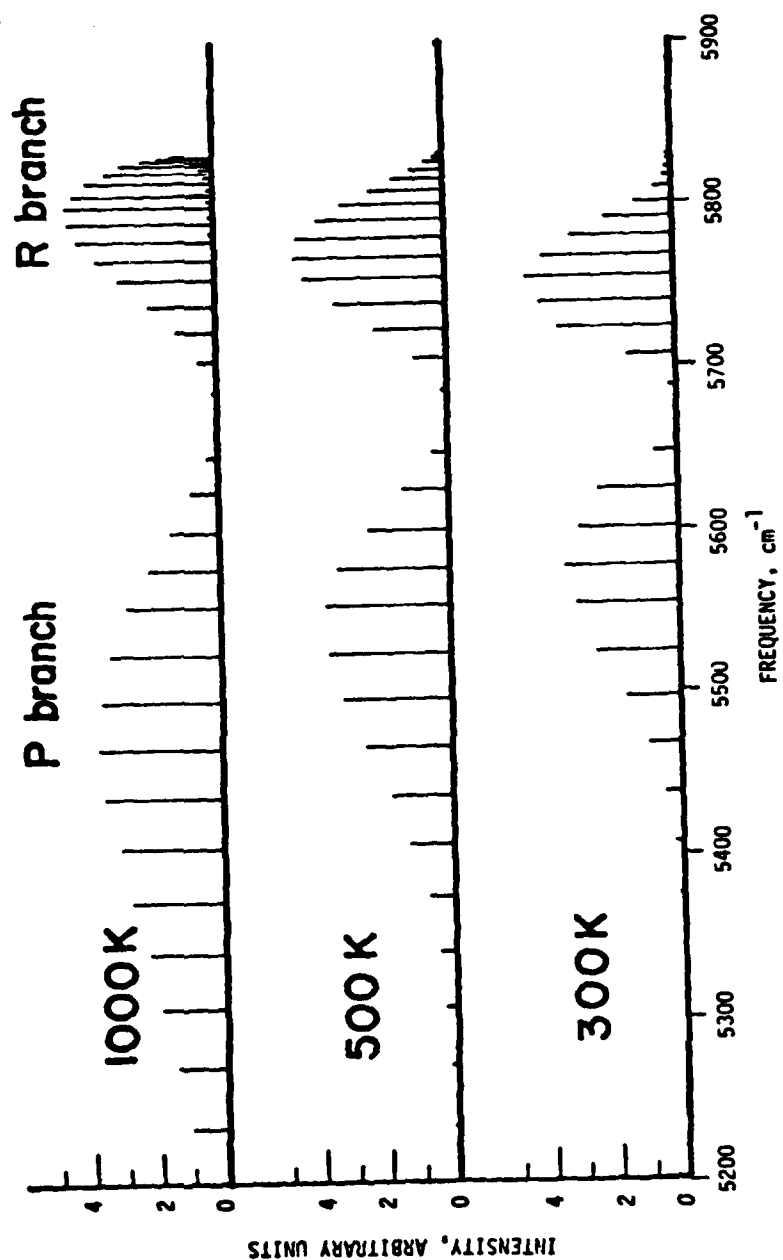


Figure 16. Calculated HCl <sup>35</sup> v=0+2 overtone spectrum. The intensity of individual levels at different temperatures can be directly compared.

In order to make more efficient use of the spatially narrow, low divergence but low powered laser beam, it was multipassed through the switch cell 6 to 8 times. Since the HCl absorption cross section at this wavelength is quite small, the beam was not significantly attenuated in the switch cell at the HCl concentration used. The number of passes were, however, limited by reflection losses at the cell windows.

Initial attempts to observe enhanced attachment were unsuccessful. Since the number of photons available at this wavelength range were so small it was decided to improve our detection sensitivity still further, even if it meant altering the operation of the switch test cell. A new anode shown in Figure 6B was added, that considerably distorted the electric fields in the switch cell, but the current to which could be more efficiently optically controlled. Conditions were also adjusted to make the switch pulses more reproducible.

Measurements were then made by averaging large numbers of switch pulses on a digital wave form analyzer both with and without the laser beam passing through the switch cell. This provided the ability to detect attachment changes of about 0.1%. Under these conditions, it appeared that we might be detecting a small amount of photo-enhanced attachment. Measurements were made with electric field intensities from 23-500 V/cm, at HCl concentrations of  $1.4 \times 10^{16}$ - $7.1 \times 10^{16}/\text{cm}^3$  and, at total switch pressures of 220 and 760 torr (some measurements were made at 220 torr to minimize collisional quenching of the excited HCl, but no observable improvement was noted). No enhanced attachment could be definitely observed during these measurements. It did appear that a small (less than 0.1%) enhancement was present during optimal laser/mixing crystal operation. Slight inconsistencies in our measurements, (probably due to changes in the laser/mixing crystal operation), however prevented a statistically meaningful determination of the presence of the much smaller than predicted

enhanced attachment rate. Thus, only an upper limit could be obtained.

Studies of HCN were conducted using similar experimental techniques and procedures to those used for HCl with a few exceptions. A portion of the  $v=0$  to 2 overtone spectrum of HCN is shown in Table 3. The much closer spacing between HCN absorption lines, compared to those of HCl, and the greater toxic hazard which prevented the safe use of the absorption cell (used for HCl to insure that the laser output was on the peak of the HCl absorption line and that it remained there) resulted in the pumping of HCN without etalons in the YAG or dye laser. While the etalon removal decreased the usable infrared power somewhat, it increased the total infrared power to 3 millijoules and broadened the line width to about  $1\text{ cm}^{-1}$ , thus making practical continuous tuning across many HCN absorption lines. Excitation of HCN was attempted at the frequencies shown in Table 3 and at electric fields of 83-5000 V/cm and at a HCN concentration of  $2.5 \times 10^{16}\text{ cm}^{-3}$ . Again, the detection of a 0.1% change in the attachment rate was possible, but no enhanced attachment was observed.



TABLE 3. HCN( $v_3=0 \rightarrow 2$ ) Transition Line and Excitation Wavelength  
From Reference 37

<u>Line</u>	<u>Position (Angstroms)</u>	<u>Excitation Range Angstroms</u>
P(2)	15348.159	15345-15353
P(5)	15369.983	15368-15372
P(23)	15521.132	15519-
P(24)	15530.554	-15534
R(4)	15300.940	15298-15303
R(8)	15276.273	15274-15278
R(14)	15242.413	15240-15244
R(18)	15221.924	-15224
R(19)	15217.061	
R(20)	15212.302	
R(21)	15207.646	
R(22)	15203.094	
R(23)	15198.646	15197-

## SECTION V

### RESULTS AND CONCLUSIONS

The results of the present study suggest that none of the gases tested appear to be good candidates for significantly improving electron beam sustained plasma switch open times via photo-enhanced electron attachment. While  $\text{NF}_3$  could not be optically pumped at its absorption peak, Figure 14 suggests that probably only a factor of 3 or less in pumping efficiency was lost. Since excitation of  $\text{NF}_3$  was performed near the two largest infrared absorption peaks and a few percent change in attachment could be detected, it appears that at least 2 or 3 orders of magnitude more photon density at the absorption peak would be required to produce a sufficient improvement in the test switch operation.

The reason that photon-enhanced attachment in  $\text{NF}_3$  was not observed is not known. However, several possibilities exist. Only the photoabsorption peak from the ground state is known and is being pumped, few of the molecules may be pumped beyond this first step. Since the wavelength used is quite long, only about 0.1 eV of energy is being imparted to the molecules when it absorbs the first photon. This is in general less than the mean electron energy in the test cell and thus the same (and additional) vibrational levels may be excited by the switch electrons. Also, even if several photons are absorbed by  $\text{NF}_3$  molecules, this additional internal energy will, in general, very quickly (on a picosecond time scale) be distributed to several different bonds thus, causing on average only a small decrease in the bond energy for any given F atom. An additional reason for not observing enhanced attachment is that of collisional quenching of the excited  $\text{NF}_3$  molecules before they are able to dissociatively attach an electron. Since the buffer gas or at

least one component of the buffer gas mixture used in the switch must have vibrational levels which can absorb energy from the conduction electrons (thereby controlling their energy distribution), it can also act as an effective quencher. Since the buffer gas must have vibrational levels at or near the mean electron energy and the attaching gas will in general have to be pumped through this level to a still higher energy state, many opportunities for near resonant energy transfer will be possible (particularly if the buffer or attaching gas is a reasonably complex molecule undergoing many collisions which further randomize the energy.) Collisional quenching could therefore result in de-excitation in a sub nanosecond time frame.

The same explanations apply even more strongly to  $C_3F_8$ . Its more complex structure provides even more bonds for the photon excitation energy to be distributed among and a greater chance for near resonant collisional quenching. Thus, it is not unreasonable that no enhanced attachment was observed.

A very large photo-absorption peak in  $C_3F_8$  was located close to some of the available  $CO_2$  laser lines. While the peak of the absorption could not be reached, the absorption cross section was still sufficiently large where  $CO_2$  laser energy was available to insure that virtually all of the  $C_3F_8$  would at least absorb a photon while in the ground state. Thus, once again, a minimum of several orders of magnitude more photon density would be required to compete with quenching and with the difficulty in ladder pumping this molecule with a  $CO_2$  laser in order for it to be of use in the switch opening process. In addition to the difficulties in observing photo-enhanced attachment in this molecule, as mentioned previously, it readily displays enhanced attachment due to the excitation and/or dissociation from the conduction electrons in the switch. It is therefore considered not to be a good candidate for photo-enhanced attachment, though it may still be useful in the switch opening process because of its electron

induced enhanced attachment.

No enhanced electron attachment could be observed in  $\text{CO}_2$ .  $\text{CO}_2$ , however, could not be effectively excited by any light sources available in our laboratory. It might be more readily excited by  $\text{CO}_2$  laser radiation if the switch gas could be considerably heated in a high current, high repetition rate switch, or if optical pumping in the 4.2-4.3 micron wavelength range were available.

Excitation of  $\text{CO}_2$  to the dissociative attachment threshold would still presumably be quite difficult, since it is not far below the photo-dissociation threshold. Ladder pumping in the infrared would require the absorption of a large number of photons for which the absorption efficiency generally increases as the molecule becomes more excited, due to the increased number of possible transitions. Thus most of the  $\text{CO}_2$  being excited will probably be dissociated before having sufficient time to dissociatively attach electrons.

Enhanced attachment in  $\text{HCl}$  could not be definitely observed using our 2 millijoule multipassed beam. If it was present, it produced a less than 0.1% change in switch current, suggesting that at least 10 joules of optical energy would be required to significantly improve switch opening times. This energy would, however, have to be supplied at a line width of less than  $0.2 \text{ cm}^{-1}$  and probably at 5 to 10 different wavelengths, since only a few percent of the  $\text{HCl}$  could be excited at any one absorption line (as shown in Figure 16) at 300K and even more wavelengths would be required at 500 or 1000K. We know of no practical way of supplying such photons and thus do not recommend direct infrared pumping of  $\text{HCl}$ .

It is believed that the reason for not observing a large photo-enhanced electron attachment in  $\text{HCl}$  might be that the cross section for  $\text{HCl}$  ( $v=2$ ) electron attachment is considerably less than that estimated by Allan and Wong.<sup>38</sup> An estimate of the

effective absorption cross section (the absorption cross section for the excitation line width used) for HCl at the excitation wavelength used is about  $1 \times 10^{-20} \text{ cm}^2$ . This value was obtained from several measurements made with various HCl/N<sub>2</sub> mixtures in the absorption cell (the same cell that was used to tune the laser output onto the HCl absorption peak but which unfortunately could not be used to determine the laser line width). Using this effective absorption cross section, a typical HCl concentration, the laser energy, and the multipass test cell geometry to calculate the amount of excited HCl formed, one finds that at least  $3 \times 10^{12} \text{ HCl}(v=2) \text{ molecules/cm}^3$  should have been present in the test region. The collisional quenching rate of HCl( $v=2$ ) by HCl( $v=0$ ) is  $1.0 \times 10^5 \text{ sec}^{-1} \text{ torr}^{-1}$ <sup>39-41</sup> which for the typical torr or less of HCl used in most of our experiments gives a quench time in the order of 10 microseconds. This is a lengthy time span in comparison to our typical observation times of less than a microsecond after excitation. An estimate of HCl( $v=2$ ) quenching by N<sub>2</sub> can be made from HCl( $v=1,3-7$ ) data,<sup>41</sup> resulting in a value of approximately  $5 \times 10^{-14} \text{ cm}^3/\text{sec}$ . For one atmosphere of N<sub>2</sub>, this suggests a quenching time of about a microsecond, which should result in a loss of no more than about half of the HCl( $v=2$ ) during our attachment measurements. For measurements made at 200 Torr, little quenching loss is expected. It therefore does not appear that a significant amount of HCl( $v=2$ ) could have been removed by quenching, which could have thus explained the lack of photo-enhanced attachment. The present results therefore suggest that the dissociative electron attachment cross section for HCl( $v=2$ ) is less than  $10^{-15} \text{ cm}^2$  (possibly by a considerable amount) throughout the range of electron field strengths studied.

No photo-enhanced attachment was observed for HCN using similar experimental techniques to those used for HCl. These results again show that at least 10 joules of tunable narrow line width radiation would be required to obtain significant enhance-

ment. The lack of enhancement shown in our present results for HCN and the chemically similar gas HCl suggest that excitation to  $v=4$  or  $5$  may be necessary in HCN before substantial enhancement is possible. This would require considerably more power, either for ladder pumping or direct excitation using an extremely small absorption cross section.

It is not believed that collisional quenching of  $\text{HCN}(v=2)$  was responsible for the lack of enhanced attachment. The self quenching rate is  $6.8 \times 10^{-12} \text{ cm}^3/\text{s}^{42}$  and quenching by  $\text{N}_2$  is  $2.6 \times 10^{-14} \text{ cm}^3/\text{s}^{42}$ , neither of which should be able to remove  $\text{HCN}(v=2)$  at a rate fast enough to prevent the observation of photo-induced attachment.

The large delays (which were beyond our control) incurred in obtaining a powerful and tunable infrared light source restricted the extent of our study of HCl and HCN. These were the only gases and excitation schemes studied that were sufficiently simple to allow a more in-depth understanding of the excitation enhanced electron attachment process. Several additional studies are thus suggested for future investigation in order to improve our understanding of the attachment process. Observations of fluorescence from the  $v=2$   $1$  state should be monitored before and after the laser fires, to insure that the calculated amount of photo-excitation was achieved, to measure and compare the rate of de-excitation with electron attachment, and to measure the amount of excitation caused by electrons. Similar studies involving pumping to other specific vibrational levels are also needed if the potentially large excitation enhanced attachments achievable with highly excited gases such as HCl and HF are to be better understood.

The results of this study suggest that the large electron attachment at the dissociative attachment threshold, particularly in HCl, may not exist. They also point out the difficulties in achieving direct infrared excitation of a molecule in competition

with collisional quenching and excitation by conduction electrons. Excitation of large numbers of molecules to highly excited states in a high pressure gas by ladder pumping is difficult and susceptible to large collisional quenching losses. Excitation to lower levels allows more direct competition by electron excitation. Two possible alternatives are recommended. Indirect excitation of simple molecules such as HF that have large vibrational steps which should help to minimize the opportunities for collisional quenching and electron excitation is suggested. Excitation to high vibrational levels, might be achieved by photo-fragmentation of a larger parent molecule or by a photo-induced chemical reaction. Secondly, excitation to an electric metastable state is suggested if an effective scheme for populating such a state can be found.

# REFERENCES

1. W. L. Morgan, M. J. Pound, 33rd Gaseous Electronics Conf. Oklahoma, OK, 1980 (derived from data of Allan and Wong).
2. W. R. Garrett, J. Chem. Phys. 71, 651 (1979).
3. B. M. Smirnov (translated by S. Chemet Edited by H. S. W. Massey) Negative Ions, McGraw-Hill (1982) pp. 24-31.
4. J. P. Ziesel, G. J. Schulz and J. Milhaud, J. Chem. Phys. 62, 1936 (1975).
5. B. M. Smirnov, "Negative Ions", McGraw-Hill (1982) p. 114.
6. R. A. Sierra, H. L. Brooks, and K. J. Nygaard, "Some Experimental Work in Gases and Gas Mixtures Used in Lasers and Ionization Detectors", Proceedings of the Second International Swarms Seminar, Oak Ridge, Tennessee, (July, 1981).
7. D. L. McCorkle, L. G. Christophorou, and S. R. Hunter, "Electron Attachment Rate Constants and Cross Sections for Halocarbons", Proceedings of the Second International Swarms Seminar, Oak Ridge, Tennessee, (July 1981).
8. Daniel W. Trainor and M. J. Boness, Appl. Phys. Lett. 32, 604 (1978).
9. J. A. Stockdale, D. R. Nelson, F. J. Davis, and R. N. Compton, J. Chem. Phys. 56, 3336 (1972).
10. D. W. Trainor and J. H. Jacob, Appl. Phys. Lett. 35, 920 (1979).
11. K. J. Nygaard, H. L. Brooks and S. R. Hunter, IEEE J. of Quantum Electronics QE15, 1216 (1979).
12. V. K. Lakawala and J. L. Moruzzi, J. Phys. D: Appl. Phys. 13, 377 (1980).
13. J. M. Wadeha, Appl. Phys. Lett. 35, 917 (1979).
14. H. M. Rosenstock, J. Phys. Chem. Ref. Data Vol. 6 Supplement 1, 742-767 (1977).



# REFERENCES (Continued)

15. E. W. McDaniel et al., Technical Report H-78-1 (1978) High Energy Laser Laboratory, US Army Missile Research and Development Command, Redstone Arsenal, Alabama 35809 Vol. II pp. 627-38, Vol. III p. 1160-62, Vol. IV p. 1863-1916.
16. F. K. Truby, Phys. Rev. 172, 24 (1968).
17. Y. Hatano and H. Shimamori, Electron Attachment in Dense Gases. Proceedings of the Second International Swarms Seminar, Oak Ridge, Tennessee (July, 1981).
18. K. D. Jordan and J. J. Wendoloski, Chem. Phys. 21, 145 (1977).
19. M. Allan and S. F. Wong, J. Chem. Phys. 74, 1687 (1981).
20. D. L. McCorkle, I. Szamrej, and L. G. Christophorou, J. Chem. Phys. 11, 5542 (1982).
21. Thermodynamic calculation done using References 3, 14, 15, 22, 23, and 24.
22. S. W. Benson, "Thermochemical Kinetics", John Wiley & Sons, 1968.
23. T. L. Cottrell, "The Strengths of Chemical Bonds", Academic Press, 1954.
24. S. W. Benson, and H. E. O'Neal, Kinetic Data on Gas Phase Unimolecular Reactions, NSRQS, NBS, 1970.
25. K. Nakamoto, "Infrared Spectra of Inorganic and Coordination Compounds", Wiley, Interscience, 1970.
26. L. M. Sverdlov, M. A. Kovner, and E. F. Krainov, "Vibrational Spectra of Polyatomic Molecules", Wiley & Sons, 1974.
27. I. W. M. Smith, J. Chem. Soc. Farad. Tras. II, 77, 2357 (1981).
28. H. J. Callomon, D. C. McKean, and H. W. Thompson, Proc. Roy. Soc., A208, 341 (1951).
29. E. L. Pace, and L. Pierce, J. Chem. Phys., 23, 1249 (1955).
30. C. Hubrich and F. Stuhl, J. Photochem. 72, 93 (1980).

# REFERENCES (Concluded)

31. J. Doucet, P. Sauvageau, and C. Sandorfy, J. Chem. Phys., 58, 3708 (1973).
32. R. E. Richton and L. A. Farrow, J. Chem. Phys., 76, 5256 (1982).
33. R. E. Scruby, J. R. Lacher, J. D. Park, J. Chem. Phys., 19, 386 (1951).
34. L. S. Rothman, A. Goldman, J. R. Gillis, R. R. Gamache, H. M. Pickett, R. L. Poynter, N. Husson, and A. Chedin, Appl. Opt. 22, 1616 (1983).
35. E. L. Pace and L. Pierce, J. Chem. Phys. 23, 1248 (1955).
36. B. J. Zwolinski (Dir) American Petroleum Institute Research Project 44, Infrared Spectral Data, Thermodynamics Research Center, Department of Chemistry, Texas A&M University, College Station, Texas (1966).
37. D. H. Rank, G. Skorinko, D. P. Eastman, and T. A. Wiggins, J. Mol. Spect. 4, 518 (1960).
38. M. Allan and S. F. Wong, J. Chem. Phys. 74, 1687 (1981).
39. S. R. Leone and C. B. Moore, Chem. Phys. Lett. 19, 340 (1973).
40. B. M. Hopkins and H-L Chem, J. Chem. Phys. 57, 3816 (1972).
41. B. M. Berquist, L. S. Dzelzkalns, and F. Kaufman, J. Chem. Phys. 76, 2984 (1982).
42. P. W. Hastings, M. K. Osborn, C. M. Sadowski and I. W. M. Smith, J. Chem. Phys. 78, 3893 (1983).

**END**

**FILMED**

**8-85**

**DTIC**